

Effect of bonding phases on the properties of Al_2O_3 based slide gate plates

A thesis submitted in partial fulfilment of the
requirements for the degree of

Master of Technology

in

Ceramic Engineering

[Specialisation: Industrial Ceramics]

by

Anil Paul

(Roll no: 212CR2439)



**Department of Ceramic Engineering
National Institute of Technology, Rourkela
ODISHA-769008**

Effect of bonding phases on the properties of Al_2O_3 based slide gate plates

A thesis submitted in partial fulfilment of the
requirements for the degree of

Master of Technology

in

Ceramic Engineering

[Specialisation: Industrial Ceramics]

by

Anil Paul

(Roll no: 212CR2439)

Under the guidance of

Dr. Bibhuti B. Nayak

Dr. Bhagirathi Mishra



**Department of Ceramic Engineering
National Institute of Technology, Rourkela
ODISHA-769008**



NATIONAL INSTITUTE OF TECHNOLOGY ROURKELA

ODISHA-769008

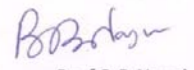
This is to certify that the thesis entitled “ **Effect of bonding phases on the properties of Al_2O_3 based slide gate plates**” submitted to National Institute of Technology Rourkela by **Mr. Anil Paul**, Roll No : **212CR2439** for the award of Master of Technology in ceramic Engineering at National Institute of Technology Rourkela is an authentic work carried out by him under my supervision and guidance. The experimental works and analysis of results are original work of the student and have not been presented anywhere for the award of a degree to the best of our knowledge.


Dr. B. Mishra

Deputy Director

DISIR, Rajgangpur

Odisha-770017


Prof. B. B. Nayak

Dept. of Ceramic Engineering

NIT Rourkela

Odisha-769008



Department of Ceramic Engineering
National Institute of Technology Rourkela
Rourkela, Orissa-769008

Declaration

I certify that

- a) The work contained in the thesis is original and has been done by myself under the general supervision of my supervisor.
- b) The work has not been submitted to any other Institute for any degree or diploma.
- c) I have followed the guidelines provided by the Institute in writing the thesis.
- d) Whenever I have used materials (experimental analysis, and text) from other sources, I have given due credit to them by citing them in the text of the thesis and giving their details in the references.
- e) Whenever I have quoted written materials from other sources, I have put them under quotation marks and given due credit to the sources by citing them and giving required details in the references.

Anil Paul

Acknowledgements

With deep regards and profound respect, I avail this opportunity to express my deep sense of gratitude and indebtedness to my supervisor Prof. B. B. Nayak, Department of ceramic Engineering, NIT Rourkela, for introducing the present research topic and for his inspiring guidance, constructive criticism and valuable suggestion throughout this research work. It would have not been possible for me to bring out this report without his help and constant encouragement.

I gratefully acknowledge Prof. S. K. Pratihara, Head of Department, Ceramic Engineering, NIT, Rourkela for giving me an opportunity to do the project work at DISIR, Rajgangpur and time to time his suggestion for the improvement of the project.

I would like to express my deep sense of gratitude and indebtedness to my co-supervisor Dr. B. Mishra (Deputy Director of DISIR). I would also like to acknowledge Dr. N. Sahoo (Director of DISIR) for their advice, supervision, and crucial contribution, which made them a backbone of this research project and so to this thesis. Their involvement with their originality have triggered and nourished my intellectual maturity that I will benefit from, for a long time to come. I also gratefully thank all the employees especially Subhasish, Harish, Lalit, Alok and all other R&D members in DISIR, Rajgangpur for their help during the course of my project work. I would like to thank Mr. R. R. Raut and Mr. Patnaik of OCL INDIA LTD for their guidance and help during my project work.

I convey my heartfelt thanks and deep gratitude to my honorable teachers Prof. S. Battacharya, Prof. S. K. Behera, Prof. R. Sarkar and all other professors of Department of Ceramic Engineering for their valuable advice, encouragement, inspiration and blessings.

Last but not the least I would like to thank Swarnima, Geeta, Ganesh, Subrato and all my classmates and my dear friends Sandeep, Snehash, Georgekutty for their encouragement and understanding. Most importantly, none of this would have been possible without the love and patience of my family. My family, to whom this dissertation is dedicated, has been a constant source of love, concern, support and strength all these years. I would like to express my heart-felt gratitude to them.

Anil Paul

anilpaul4365@gmail.com

ABSTRACT

Recent technological advances in steelmaking process demand higher hot strength and longer life of various supporting components by economical means. Flow control refractories like slide gate demands superior thermal and thermo-mechanical properties apart from corrosion to different grade of steel. During operation the slide gate plates are subjected to severe thermal shock, erosion with steel stream, corrosion with deoxidiser used and abrasion with respect to infiltrated material and among the plate itself. The superior thermal shock resistance coupled with better resistance to corrosion and erosion paves way for carbon bonded slide gate plates. Moreover Alumina and carbon bonded plates are more popular which can stand abusive condition generated during casting of different grade of steel.

In the present work different quality of alumina are taken along with different metals as the starting materials. Different compositions are formulated taking single or combination of metals which are mixed with phenol formaldehyde resin and pressed with a specific pressure of 2000kg/cm^2 . The bricks are cured at 240°C for 12 hours. Physical, thermal and thermo mechanical properties are evaluated. Also the bricks are fired at 1100°C in reducing atmosphere. Physical, thermal and thermo mechanical properties are evaluated and correlated with the mineralogical and microstructural analysis. Based on these findings carbon bearing plates are made with the addition of carbon black or carbon black and graphite. The addition is restricted up to 5%. Properties are evaluated and correlated with mineralogical and microstructural analysis. Plates containing aluminium metal shows superior thermal and thermo-mechanical properties than silicon metal containing Al_2O_3 slide plates. However plate containing metal in combination has the best thermal and thermo-mechanical properties. Fused alumina based plates has comparatively superior properties for all grade of metal addition. Plate containing both carbon black and graphite flake was having comparatively efficient properties in carbon bonded slide plates.

To improve the thermal shock resistance, corrosion resistance and oxidation resistance, along with mechanical properties, *in situ* synthesised plasma fused $\text{ZrO}_2\text{-SiC}$ was incorporated in the $\text{Al}_2\text{O}_3\text{-C}$ slide gate plates. Apart from mechanical properties, thermal spalling resistance, erosion resistance and oxidation resistance of these slide plates were compared with the normal ones.

The metal bonded slide gate plates are fired in 1600°C in nitrogen atmosphere for forming nitride bonds. These nitride bonded slide plates were giving significant enhancement in properties and it can be a suitable substitution for all the carbon bonded slide gate plates.

Contents

Certificate.....	iii
Declaration.....	iv
Acknowledgement.....	v
Abstract.....	vi
Contents.....	vii
List of figures.....	x
List of tables.....	xii
1. Introduction.....	1
1.1 Background.....	2
1.2 Slide gate plates.....	2
1.2.1 Refractory requirement for slide gate plates.....	3
1.2.2 Why $\text{Al}_2\text{O}_3\text{-C}$ refractories for Slide gate plates?.....	3
1.3 Raw materials for $\text{Al}_2\text{O}_3\text{-C}$ refractories.....	4
1.3.1 Role of carbon.....	4
1.3.2 Role of binder.....	4
1.3.3 Role of antioxidant.....	4
1.4 Problems in $\text{Al}_2\text{O}_3\text{-C}$ refractories.....	5
1.5 Synthesis of $\text{ZrO}_2\text{-SiC}$ by plasma fusion.....	5
1.6 Scope and character of present work.....	6
2 Literature review.....	7
2.1 Additives in $\text{Al}_2\text{O}_3\text{-C}$ refractories.....	8
2.1.1 Enhancement of thermo-mechanical properties and oxidation resistance.....	8
2.1.2 Erosion and corrosion resistance.....	9
2.2 Effect of different carbon sources on $\text{Al}_2\text{O}_3\text{-C}$ refractories	11
2.3 Effect of nano scaled additives.....	12
2.4 Effect of $\text{ZrO}_2\text{-SiC}$ in $\text{Al}_2\text{O}_3\text{-C}$ refractories.....	13
2.5 Effect of Sialon formation in $\text{Al}_2\text{O}_3\text{-C}$ refractories.....	14
3 Objectives of present work	15
4 Experimental works	17
4.1 Specification of raw materials	18

4.2 Fabrication of Al ₂ O ₃ based slide plates	18
4.2.1 Batch preparation	18
4.2.2 Mixing	20
4.2.3 Ageing	20
4.2.4 Pressing	21
4.2.5 Tempering	21
4.2.6 Coking	21
4.3 General characterisation of Al ₂ O ₃ refractory	21
4.3.1 Physical properties	21
4.3.1 .1 Apparent Porosity and bulk density	21
4.3.1 .2 Cold crushing strength	22
4.3.2 Mechanical and Thermo mechanical properties	22
4.3.2 .1 Modulus of rupture & Hot modulus of rupture	22
4.3.3 Thermal and Thermo chemical properties	23
4.3.3 .1 Thermal shock resistance	23
4.3.3 .2 Erosion resistance	23
4.3.3 .3 Oxidation resistance	24
4.3.3 .4 Phase analysis by X-ray diffraction	24
4.3.3 .5 microstructural analysis	24
4.3.3 .5.1 Optical microscopy/SEM/FESEM/EDS	24
5. Result and Discussions	25
5.1 Metal bonded Al ₂ O ₃ slide plates	26
5.1.1 Physical properties	26
5.1.2 Mechanical and Thermo mechanical properties	27
5.1.2 .1 Modulus of rupture & Hot modulus of rupture	27
5.1.3 Structural properties	29
5.1.4 microstructural analysis	30
5.1.4.1 Optical microscopy/SEM/FESEM/EDS	30
5.2 Carbon bonded Al ₂ O ₃ slide plates	33
5.2.1 Physical properties	33
5.2.1.1 Apparent Porosity, bulk density, Cold Crushing Strength	33
5.2.2 Mechanical and Thermo mechanical properties	34

5.2.2 .1 Modulus of rupture & Hot modulus of rupture	34
5.2.3 Micro Structural properties	35
5.3 ZrO ₂ -SiC bonded Al ₂ O ₃ -C Slide plates	37
5.3.1 Physical properties	37
5.3.1.1 Apparent porosity, bulk density and cold crushing strength	37
5.3.2 Mechanical and Thermo mechanical properties	38
5.3.2 .1 Modulus of rupture & Hot modulus of rupture	38
5.3.3 Oxidation resistance	39
5.3.4 Thermal shock resistance	41
5.3.5 Erosion resistance	41
5.4 Nitride bonded Al ₂ O ₃ Slide plates	43
5.4.1 Physical properties	43
5.4.1.1 Apparent porosity, bulk density	43
5.4.2 Structural and microstructural properties	44
5.4.2 .1 Structural properties	44
5.4.3 Thermo mechanical properties	46
5.4.3 .1 Hot modulus of rupture	46
5.4.3 .2 microstructural Structural properties	47
5.4.3.2.1 FESEM (Mapping)	47
6. Conclusions and Scope of future work	48
References	51

List of Figures

Fig. No.	Figure description	Page No.
Fig. 1.1	Schematic diagram for liquid steel casting equipment	3
Fig. 1.2	Schematic diagram for Plasma furnace	5
Fig. 4.1	Mixing sequence for Al ₂ O ₃ based refractory	20
Fig. 4.2	Schematic representation of compressive testing setup	22
Fig. 4.3	Schematic representation of 3 point bending test	22
Fig. 5.1	Variation of AP (a), BD (b) and CCS (c) of different tempered and coked samples	26
Fig. 5.2	Variation of MOR for the samples cured at 240 °C and fired at 1100 °C for 6h in coke environment.	28
Fig. 5.3	Variation of HMOR for the samples cured at 240 °C and fired at 1100 °C for 6h in coke environment.	28
Fig. 5.4	XRD patterns of Al ₂ O ₃ samples tempered at 240 °C and coked at 1100 °C	29
Fig. 5.5	Optical image of sample T-3, (a) before and (b) after coking	30
Fig. 5.6	FESEM micrograph of sample T- 3 at tempered state (a); SEM micrograph of sample T- 3 at coked state (b) and EDS analysis of sample T- 3 at coked state (c)	31
Fig. 5.7	FESEM micrograph of coked sample: (a) T-1, (b) T- 2, (c) T-4 and (d) T-5.	32
Fig. 5.8	Variation of (a) apparent porosity, (b) bulk density and (c) CCS of carbon bonded samples.	34
Fig. 5.9	Variation in (a) MOR and (b) HMOR of carbon bonded samples	35

Fig. 5.10	FESEM micrographs of coked sample (a) T-6, (b) T-7, (c) T-8, and (d) T-9	36
Fig. 5.11	Variation in (a) AP (b) BD and (c) CCS of coked T-7 samples as a function of ZrO ₂ -SiC	37
Fig. 5.12	MOR (a) and HMOR (b) as a function of wt % ZrO ₂ -SiC in Al ₂ O ₃ -C	39
Fig. 5.13	Images of oxidation resistance of ZrO ₂ -SiC added Al ₂ O ₃ -C samples	40
Fig. 5.14	Oxidation index as a function of wt % of ZrO ₂ -SiC in Al ₂ O ₃ -C sample	40
Fig. 5.15	Variation in Erosion resistance by addition of ZrO ₂ -SiC in Al ₂ O ₃ -C sample	41
Fig. 5.16	Erosion index as a function of wt % of ZrO ₂ -SiC in Al ₂ O ₃ -C sample	42
Fig. 5.17	Variation in (a) AP and (b) BD of Al ₂ O ₃ samples fired under N ₂ atmosphere.	43
Fig 5.18	XRD patterns T-1, T-2, T-3, T-4 and T-5 fired at 1600°C in N ₂ atmosphere	45
Fig 5.19	Variation in HMOR for samples T-1, T-2, T-3, T-4 and T-5 fired at 1600°C in Nitrogen atmosphere	46
Fig 5.20	FESEM micrograph (a), EDS Mapping (b) of sample T-3	47

Fig. 5.25	Variation in oxidation index by addition of ZrO ₂ -SiC in Al ₂ O ₃ -C sample	49
Fig. 5.26	Images showing variation in Erosion resistance by addition of ZrO ₂ -SiC in Al ₂ O ₃ -C sample.	51
Fig. 5.27	Variation in Erosion index by addition of ZrO ₂ -SiC in Al ₂ O ₃ -C sample	51
Fig. 5.28	Variation in (a)AP and (b) BD of samples T-1, T-2, T-3, T-4 and T-5 fired at 1600°c in Nitrogen atmosphere	53
Fig. 5.29	variation in HMOR of samples T-1, T-2, T-3, T-4 and T-5 fired at 1600°c in Nitrogen atmosphere	54
Fig. 5.30	XRD patterns T-1and T-3 fired at 1600° c in Nitrogen atmosphere	55
Fig. 5.31	XRD patterns T-2 and T-4 fired at 1600° c in Nitrogen atmosphere	55
Fig. 5.32	XRD patterns T-5 fired at 1600°c in Nitrogen atmosphere	56
Fig 5.33	(A) FESEM micrograph (B) FESEM Mapping, of sample T-3 fired at 1600°c in Nitrogen atmosphere .	57

List of Tables

Table no	Description	Page no
Table 4.1	Specification of raw materials for Al_2O_3 refractory	18
Table 4.2	Different recipes of Al_2O_3 refractory for slide plates. [TA stands for tabular alumina and WFA stands for white fused alumina]	19
Table 4.3	Different recipes of Al_2O_3 - C refractory for slide plates. [TA stands for tabular alumina and WFA stands for white fused alumina]	19
Table 4.4	Different recipes of Al_2O_3 - C- ZrO_2 -SiC refractory for slide plates. [TA stands for tabular alumina and WFA stands for white fused alumina]	20
Table 5.1	Variation in Erosion depth and Erosion index by addition of ZrO_2 -SiC	41

Chapter -1
Introduction

Introduction

1.1: Background of present work

In recent years, according to the changing trends in steel making, the demand for high performing shaped refractories are increasing. Al_2O_3 -C refractories are widely used in the continuous casting of steel ^[1]. Especially in the fabrication of slide plates these refractories are the most suitable ones because of their better corrosion resistance and thermal shock resistance. Also the high flexural and compressive strength, low thermal expansion, high thermal conductivity, low modulus of elasticity, resistance to molten metal and slag are some characteristic features of Al_2O_3 -C refractories ^[2,3].

Oxidation and subsequent deterioration of properties at high temperature is the main drawback as far as Al_2O_3 -C refractories are concerned. Such oxidation problem can be reduced by the use of antioxidants and also by minimising the amount of carbon addition ^[4].

Till now the most popular antioxidants used in industry are Al and Si, because of their low cost and acceptable performance. The formation of Aluminium carbide phase in Al added samples resulted in good oxidation resistance ^[5, 6]. Formation of SiC is the major reason for oxidation resistance in Si added samples ^[4].

Enhancement in properties of Al_2O_3 based refractories for slide plates are of major concern. Different approaches to attain this target are by varying the antioxidants, varying the carbon sources, introducing new antioxidants and varying the bonding phases ^[7-9]. These approaches have been tried in this present work for optimisation.

1.2: Slide Gate plates

Ladle slide gate plates are critical flow control components in steel making process. As shown in the Figure 1.1, slide gate plates control the flow of steel from steel ladle to tundish. Since they are in contact with hot liquid steel, hot strength properties of the refractories used for slide plate should be given greater importance.

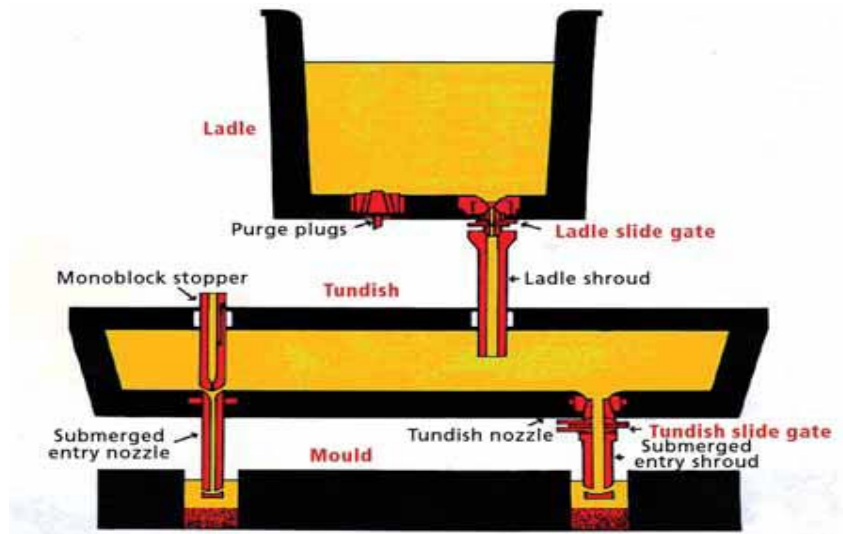


Fig1.1 Schematic diagram for liquid steel casting equipment ^[10].

1.2.1 Refractory requirement for slide gate plates

Since liquid steel is flowing through slide plates they are subjected to erosion, especially by the attack of slag. Because of the sliding of the plates, abrasion resistance is an area of concern. Since it is in contact with molten steel at high temperature, high hot strength is required. Load bearing capability is also matter of concern. The refractory requirements for slide gate plates are,

- High thermal shock resistance
- Erosion resistance to metal slag
- Low coefficient of thermal expansion
- High thermal conductivity
- Good crushing strength
- Abrasion resistance

1.2.2 Why $\text{Al}_2\text{O}_3\text{-C}$ refractories for Slide gate plates?

Most of the refractory requirements for slide plates which are mentioned above are satisfied by $\text{Al}_2\text{O}_3\text{-C}$ refractories. The presence of carbon gives them good resistance to abrasion, corrosion and thermal spalling. Carbon has non-wettability property which prevents the infiltration of metal and slag to the system. Also carbon will improve the thermal shock resistance of the material. $\text{Al}_2\text{O}_3\text{-C}$ refractories are having good flexural

and compressive strength at high temperature which prevents erosion by molten steel and slag. Apart from these properties $\text{Al}_2\text{O}_3\text{-C}$ has high thermal conductivity and low coefficient of thermal expansion resulting in high resistance to thermal spalling. Good affordability assisted by afore mentioned properties make $\text{Al}_2\text{O}_3\text{-C}$ a potential candidate flow control refractories in Iron and steel industries.

1.3: Raw materials for $\text{Al}_2\text{O}_3\text{-C}$ refractories

Primary raw material for making $\text{Al}_2\text{O}_3\text{-C}$ refractories are high purity sintered/tabular or fused alumina with or without addition of other synthetically prepared materials like mullite/zirconia/spinel. The main carbonaceous materials are carbon black or high purity graphite. Apart from these materials it contains antioxidant in form of metallic/metal carbide or metal boride powders.

1.3.1 Role of carbon

The addition of carbon imparts high thermal conductivity, low coefficient of thermal expansion and non wetting properties. It has following advantages when added to $\text{Al}_2\text{O}_3\text{-C}$.

1. High resistance to thermal spalling
2. High resistance to abrasion.
3. High resistance to erosion and corrosion

It minimizes the contact between the slag and refractory ^[11]

1.3.2 Role of binder

Binders provide green strength to the materials. Normally the binders used in $\text{Al}_2\text{O}_3\text{-C}$ refractories are phenolic formaldehyde resin. It imparts excellent strength after drying with the formation of resite and also after firing in reducing condition with the formation of carbon bond, but it has a disadvantage of lower oxidation resistance than other form of carbon ^[11, 12].

1.3.3 Role of antioxidant

The functions of antioxidant are,

1. They have high affinity for oxygen, preventing oxidation of carbon.
2. They forms carbide with carbon

1.4: Problems in $\text{Al}_2\text{O}_3\text{-C}$ refractories

1. Carbon will get oxidised at temperatures above 500°C in oxidising condition resulting in loss of strength, increase of porosity leading to poor corrosion and erosion resistance.
2. Dissolution of alumina by metal slag or oxidation of carbon by iron oxide in slag or penetration of slag into the pores leads to erosion.

To overcome the above problems, $\text{ZrO}_2\text{-SiC}$ additives may be used in $\text{Al}_2\text{O}_3\text{-C}$ refractories. In this work, plasma synthesized $\text{ZrO}_2\text{-SiC}$ powders have been used for improving the properties of $\text{Al}_2\text{O}_3\text{-C}$ refractories.

1.5: Synthesis of $\text{ZrO}_2\text{-SiC}$ by plasma fusion

$\text{ZrO}_2\text{-SiC}$ was prepared synthetically by fusing zircon and carbon in an export arc 20 KW plasma furnace. Argon was used as ionising gas. Total fusion time was 45 minutes. Temperature of fusion was around 3000°C . Schematic diagram is given in Fig 1.2.

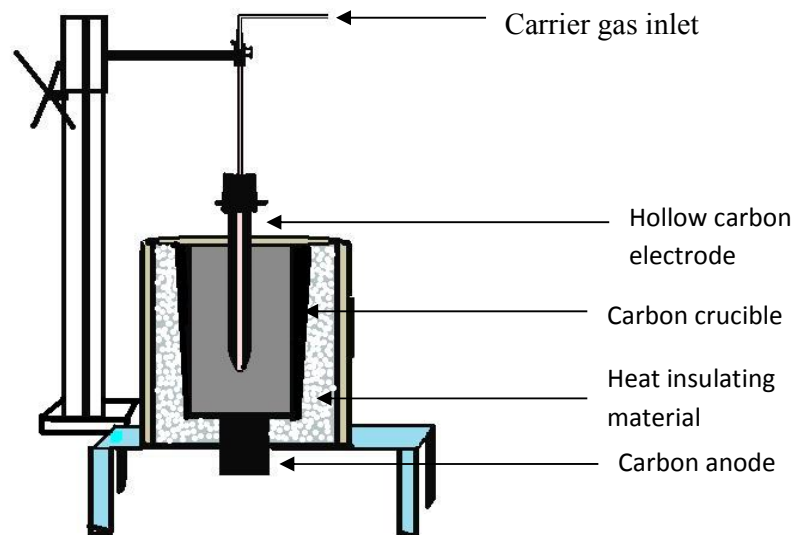
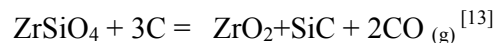


Fig1.2 Schematic diagram for Plasma furnace.

Plasma fused ZrO₂-SiC is synthesized by carbo-thermal reduction of Zircon sand. It depends on the amount of carbon added.



This ZrO₂-SiC was used as an antioxidant in the present work.

1.6 Scope and character of present work.

This thesis work includes 8 chapters. Chapter-1 deals with the background of the work and introduction to refractories. The chapter 2 includes the literature review on the effect of different additives on the Al₂O₃ based refractory samples. The objective of this work is mentioned in the chapter 3. The detailed explanation of the experimental part is given in chapter 4. Manufacturing method, methods used to evaluate the properties etc. are briefly explained. The results and discussion was described in the chapter 5. Chapter 6 gives the conclusions made from the results obtained and scope of future work. References are given at the end of this thesis.

Chapter -2
Literature Review

2. Literature Review

2.1 Additives in Al₂O₃-C refractories

The most common additives in Al₂O₃-C refractories are Al and Si. They are having acceptable performance and are economical ^[4]. For improving corrosion resistance and hot strength ZrO₂ is added to Al₂O₃-C refractories. To attain different properties, different additives are tried, like silica and microsilica are added in combination to improve toughness and mechanical strength ^[14]. The nano scaled additives, graphene nano sheets, multi walled carbon nanotubes etc. are also applied in Al₂O₃-C refractories and they are showing appreciably good results.

2.1.1 Enhancement of thermo-mechanical properties and oxidation resistance.

Oxidation is the main problem as far as carbon based Al₂O₃ refractories is concerned. The remedy or solution for that problem is the use of antioxidants. Al and Si are the usual antioxidants considering the economical factor and the results. J. Javadpour *et al.* ^[4] reported that aluminium presence has considerable effect on the mechanical and physical properties of Al₂O₃-C refractories. They added that properties may change with the temperature, i.e. degradation of properties at higher temperature is reported. The formation of SiC in Si containing samples is the basic reason for the better mechanical properties and oxidation resistance ^[15, 16]. In Al containing samples the formation of Aluminium carbide and nitride improved the oxidation resistance of the sample. But at higher level Si addition SiO₂ layer formed at the surface blocks the further increase in oxidation resistance. At higher temperature the amount of aluminium carbide decrease and it eventually decreases the strength of the refractory.

Liu Qing-Cai *et al.* ^[17] investigated on the addition of ZrO₂ in Al₂O₃-C refractories. They reported that it increases the oxidation resistance of the refractory. The presence of ZrO₂ also improves the mechanical strength of the refractory.

For Al₂O₃-C refractories carbon nano tubes (CNTs) are excellent reinforcements. But they will react with the gaseous phases like Si (g), SiO (g), Al (g) or they may react with antioxidants. So multi walled carbon nano tubes and polycarbosilane (PCS) are mixed with micro alumina powder and then applied in Al₂O₃-C refractories. Luo *et al.*

^[18] reported that the mechanical properties of $\text{Al}_2\text{O}_3\text{-C}$ refractories were improved greatly with addition of polycarbosilane (PCS) due to the more homogenous dispersion of multi-walled carbon nanotubes (MWCNT) as well as more residual MWCNTs. Meanwhile, the oxidation resistance of $\text{Al}_2\text{O}_3\text{-C}$ refractories with PCS was improved greatly, which was supposed that the in situ formed SiC_xO_y coating prevented the oxidation of MWCNTs to some extent. As well, the SiC_xO_y coating could greatly strengthen the interfacial bond between MWCNTs and matrix, which also gave a benefit to the mechanical properties.

The addition of $\text{ZrO}_2\text{-SiC}$ in $\text{Al}_2\text{O}_3\text{-C}$ refractories significantly improves its thermal shock resistance, oxidation resistance and hot strength. Bei-yue *et al.* ^[19] reported that the crushing strength, thermal spalling resistance and density of the refractory have been improved by the addition of $\text{ZrO}_2\text{-SiC}$. Silicon, microsilica and their combination are also used as additives for $\text{Al}_2\text{O}_3\text{-C}$ refractories. Fan *et al.* ^[14] investigated the addition of silicon, microsilica and their combination in $\text{Al}_2\text{O}_3\text{-ZrO}_2\text{-C}$ refractories. They reported that silicon enhanced the mechanical strength and microsilica on the other hand improved the toughness. They further reported that the combination of micro silica and silicon had better results as it improved the toughness and strength simultaneously. The reason behind these results might be the formation of SiC whiskers from silicon and the formation of mullite (needle like) from microsilica.

2.1.2 Erosion and corrosion resistance

The investigation of reaction kinetics between molten metal and $\text{Al}_2\text{O}_3\text{-C}$ refractories with silicon additive were done by SASAI *et al.* ^[20]. They reported that the rate of reaction between the molten steel and refractory was controlled by diffusion of the CO gas and SiO gas through the pores in oxide film formed at the interface of refractory and molten steel. The rate of the reaction between the molten steel and refractory was dependent on the grade of steel. They reported that in the Ti-killed molten steel the reaction was faster than in the Al-killed molten steel. For the refractory immersed in Ti-killed molten steel, the reaction is fast because the surface of refractory was covered discontinuously by porous oxide film. But in Al-killed molten steel, the refractory surface was covered by a dense oxide film, hence the rate of reaction is slower.

The erosion resistance of $\text{Al}_2\text{O}_3\text{-C}$ refractories are improved by addition of ZrO_2 . corrosion happens in the refractory because of the interaction between the refractory and the melt. It leads to dissolution of the refractory into the melts. Liu *et al.* ^[17] investigated that ZrO_2 improves the corrosion resistance of the refractory. The corrosion rate of both AZ and AC system refractories increased with the temperature of the molten bath and iron oxide content of the melts. The corrosion rate of the rotary test was 30% higher than the corrosion rate of quasi-stationary immersion test. First graphite oxidation and then deteriorative layer formation, this is the corrosion mechanism in Alumina carbon refractories in smelting reduction melts with iron. Corrosion mechanism for the AZ refractory was the interaction between melts and refractory and the dissolution of the refractory constituents into the melts. They reported that the new compounds FeSiO_3 , ZrSiO_4 , Ca_3FeO_4 CaSiO_3 were formed in the deteriorative layer during the interaction between Alumina Zirconia refractory system and the melts.

In smelting reduction with iron bath the conditions are much more complex compared with that of blast furnace. The corrosion behaviour of refractories are different for blast furnace and smelting reduction with iron bath ^[21, 22]. Liu *et al.* ^[17] explained the corrosion rate of ZrO_2 added $\text{Al}_2\text{O}_3\text{-C}$ in different slag test.

Corrosion rates of $\text{Al}_2\text{O}_3\text{-C-ZrO}_2$ refractories (g/h), at 1790 K.

ZrO_2 (%)	0.11	1.5	3	6	9
Quasi state	1.24	1.15	1.02	0.93	0.89
Rotary test	1.63	1.62	1.31	1.27	1.12
BF	0.68	0.69	0.65	0.66	

The percentage of ZrO_2 in $\text{Al}_2\text{O}_3\text{-C-ZrO}_2$ refractories is usually 6-9%. From the table it is clear that higher the amount of ZrO_2 lower is the corrosion rate of refractories. Corrosion rate in rotary test around 30% more than corrosion rate in quasi state immersion test.

The corrosion resistance of the $\text{Al}_2\text{O}_3\text{-C}$ refractories can be improved by the addition of CaB_6 , Boron carbide (B_4C) and $\text{Al}_2\text{O}_3\text{-C-SiC}$ composite the synthesized from clay ^[23-25]. In addition, ZrO_2 and Sic powders also improve the properties of the $\text{Al}_2\text{O}_3\text{-C}$ refractories because of their high toughness and corrosion resistance ^[26, 27].

2.2 Effect of different carbon sources on $\text{Al}_2\text{O}_3\text{-C}$ refractories

Carbon containing refractories are widely used in metallurgical industries as functional and high duty refractories since they are having excellent thermal, chemical and mechanical properties. Major advantage of carbon is its low wetting nature with molten slag, which helps in providing high erosion resistance. It is also having high thermal conductivity, which makes it efficient in the case of thermal shock resistance [28-31]. Carbon will react with additives Al or Si to form carbide phases such as Al_4C_3 , SiC, $\text{Al}_4\text{O}_4\text{C}$ and Al_4SiC_4 , it improves toughness and strengthens the material giving better mechanical properties [32, 33]. Different carbon sources generally used for $\text{Al}_2\text{O}_3\text{-C}$ refractories are carbon black, graphite flake and also phenolic resin can be considered as a carbon source. Fan *et al.* [11] reported that different morphologies of SiC can be produced by reaction between different carbon sources and Si metal powder. When carbon black is used as carbon source it forms spherical SiC particles, graphite flakes forms SiC whiskers and derivative carbon which was pyrolysed from phenolic resin, also forms SiC whiskers.

The formation of SiC phase in the matrix has positive effect on the mechanical properties of the refractory. At 1000 °C the bonding was only by carbon derived from phenolic resin hence there was not much variation in mechanical properties of both the refractories with different carbon sources. When temperature increases, SiC phase was formed in the matrix. In graphite flake containing refractories larger displacement and also greater force can be observed, compared with refractories with carbon black. It is due to the sliding mechanism within graphite layers and the formation of more curved SiC whiskers in the refractories containing graphite flakes. And this sliding mechanism which is operating between the graphite layers would lead to the apparent tortuosity of cracks [31]. Also there would be an enhancement in the load transfer mechanism because of the generation of larger specific surface area [34]. And according to the morphology of SiC, SiC whiskers are providing better mechanical properties than SiC particles, especially based on the toughening mechanisms like crack deflection, pull out, whisker bridging and whisker fracture in SiC whiskers [11, 35].

Usually phenolic resin is very efficient binder in $\text{Al}_2\text{O}_3\text{-C}$ refractories because it has many properties like high fixed carbon rate, and it has good wettability with graphite and oxide. But, phenolic resin changes to isotropic glassy carbon during the heating process. Then it will become more brittle and increases thermal stress in the material. In addition to that, gaseous products like CO, CO_2 , CH_4 , C_2H_6 , and H_2O are

released during transformation of the organic groups, and it deteriorates the microstructure of the refractory materials [36-40]. For accelerating the formation of graphite structure from various carbon sources transition metals like nickel, iron and cobalt are used as catalysts. Luo *et al.* [41] investigated on Ni catalysed phenolic resin as binder for Al₂O₃-C refractories. In the case of as-received phenolic resin only amorphous carbon was formed, but in the case of Ni-catalyzed phenolic resin when pyrolysis temperature increased from 450 °C to 1050 °C crystalline graphite carbons were obtained, specifically gradual formation of multi-walled carbon nanotubes (MWCNTs) were reported. According to the coking temperature morphology and the quantity of carbon nanotubes (CNTs) formed varies. Because of the formation of these carbon nanotubes the mechanical properties of refractories with Ni-catalysed phenolic resin were significantly improved.

Ultrafine microcrystalline graphite can be used as a replacement for graphite flakes in Al₂O₃-C refractories. High energy ball milling of natural microcrystalline graphite along with α -Al₂O₃ powders (micron sized) will yield ultrafine microcrystalline graphite (UMCG) powders. Wang *et al.* [42] reported that the mechanical properties like modulus of elasticity (MOE), cold modulus of rupture (CMOR), force and displacement of Al₂O₃-C refractories with Ultrafine microcrystalline graphite (UMCG) powders were improved compared with those refractories without UMCG. The microstructural evolution of Al₂O₃-C refractories are affected by the addition of UMCG. Formation of SiC whiskers, AlN and Al₄C₃, were accelerated by the presence of UMCG, because compared with graphite flakes they are having higher reactivity.

2.3 Effect of nano scaled additives

Aneziris *et al.* [43] and Luo *et al.* [44] investigated and found that Al₂O₃-C refractories with carbon nanotubes (CNTs) have better mechanical properties than those refractories without CNTs. Other nanosized carbon source, graphene oxide nanosheets (GONs) had attained much attention in ceramic matrix composites due to their excellent properties, especially physical, chemical and mechanical [45-47].

By the addition of GONs, refractories could be prepared with excellent mechanical properties and thermal spalling resistance [48,49]. The GONs are having high specific surface and also high reactivity, so that it reacts with other additives easily (Al and Si powder) forming ceramic whiskers. These whiskers reinforce the refractories and provide toughness [50, 51]. Luo *et al.* [44] reported that the use of multi walled carbon nano tubes (MWCNTs) in Al₂O₃-C refractories increased the mechanical properties in

the firing temperature range from 800 to 1200°C, but it dramatically decreased at 1400 °C. The refractories containing 0.05 wt% MWCNTs showed better mechanical properties than those with only graphite flake. But the properties showed deterioration when the amount of MWCNT increased from 0.1 to 1 wt%. The strengthening and toughening mechanism of MWCNTs and formation of large number of ceramic phases at 800 and 1000 °C, were the reasons behind the improvement in mechanical properties. At 1200 and 1400 °C, the reason for improvement was the morphology and quantity of SiC whiskers induced from MWCNTs. At higher amount of MWCNTs the mechanical properties got deteriorated in the sample because of agglomeration of MWCNTs. Wang *et al.*^[52] reported that compared to graphite flakes, graphene oxide nanosheets are having higher reactivity, because of that, at lower temperature more ceramic whiskers are formed by GONs. At 800 °C graphene oxide nano sheets are having strengthening effects .At 1000-1400 °C it is having strengthening effect with the whiskers formed and the graphite flake. Because of these strengthening effects the mechanical properties are improved.

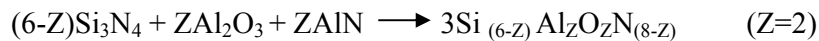
2.4 Effect of ZrO₂-SiC in Al₂O₃-C refractories.

If high temperature resistance, good fracture strength and better corrosion resistance are required for the refractories, ZrO₂ and SiC are the better choice of materials which can provide such properties. An efficient method for producing various non-oxide products is carbo-thermal reduction, and ZrO₂- SiC can be produced by this method. Kljajevi *et al.*^[13] investigated on carbo-thermal reduction for synthesis of ZrO₂- SiC . Adding zircon powder and carbon black in the apparatus, heat treatment in argon atmosphere has been carried out. The m-ZrO₂, t-ZrO₂ or ZrO₂-SiC can be formed according to the ratio of C/ZrSiO₄. When Zircon and carbon are heated in argon atmosphere in the furnace the powder which is synthesized contained ZrO₂ and SiC as 87.7% & 16.3% respectively. Yu *et al.*^[19] reported that by incorporating ZrO₂- SiC in Al₂O₃-C refractories would increase the properties like crushing strength, bulk density and thermal spalling resistance. They reported that as the percentage of ZrO₂-SiC increases bulk density also increases. Because of toughness of ZrO₂ and SiC cold crushing strength also increases. But when more additive is added micro flaws will become larger and also the difference in thermal expansion coefficient between the refractories and the additives increases. So crushing strength decreases. During cooling there would be volume change because of the phase transformation reaction of ZrO₂ and

it brings micro flaws to grain boundary. Tips and edges of the flaws can be cut short, so that they won't extend to break the material. And hence it increases thermal spalling resistance.

2.5 Effect of Sialon formation in Al₂O₃–C refractories

In Al₂O₃–C refractories, carbon will provide corrosion resistance to some extent, but oxidation of carbon is a major problem. So, additives like Al and Si are added to prevent oxidation. AlN in the form of short columns and SiC whiskers may generate in Al₂O₃–C refractories if Al and Si are added as additives, respectively. AlN will enhance hot modulus of rupture, but thermal shock resistance is very poor. In the similar way, SiC whiskers increases thermal spalling resistance, but hot modulus of rupture is very poor. So, Zhu *et al.* ^[53] investigated that when both Si and Al were added as additives and nano sized Ni was used as catalyst β -Sialon formation was found with plane structure. Diffusion of Al and Oxygen into silicon nitride lead to the formation of β -Sialon. Hot modulus of rupture increased because of the β -Sialon presence. β -Sialon improved the thermal spalling resistance and hot strength of the refractory. Li *et al.* ^[54] reported that at 1500 °C O-Sialon whiskers were synthesized and it enhanced the strength of Al₂O₃–C refractories at high temperature. It was because the particle and matrix was tightly interlinked by the whiskers. Fracture strength of the refractories were improved, and also because of the presence of large diameter whiskers thermal spalling and oxidation resistance improved significantly. Gibbs free energy reactions are lower for Al metal, so it will react with surrounding atmosphere like nitrogen/oxygen/carbon easily or early as compared with Si metal. The nitridation or carbonisation of Si metal won't happen until the temperature reaches around 1000 °C. Silicon nitride will be stable when partial pressure of nitrogen is more. Sialon was formed from the reaction between Alumina and the nitrides,



It is difficult to form β -Sialon without high partial pressure of nitrogen. Because Si will easily form SiC and for forming silicon nitride high partial pressure of nitrogen is required. So they were using nano sized Ni as catalyst, and at low nitrogen pressure this catalyst enhanced the nitridation of Si, and the diffusion of AlO into Si₃N₄ is accelerated and hence it enhances the formation of β -Sialon in planar structure. They reported that Sialon improved the oxidation resistance also, even oxidation of sialon will lead to the formation of mullite which also provides ceramic bonding.

Chapter -3
Objectives of present work

Slide gate plate is a vital component of flow control refractories. To have trouble free operation of slide gate plate proper understanding of refractories is of paramount importance to develop $\text{Al}_2\text{O}_3\text{-C}$ plates with superior mechanical, thermo-mechanical and pyro chemical properties to sustain these stresses during use.

In the present work, metal bonded Al_2O_3 , carbon bonded Al_2O_3 with optimised addition of anti oxidants with or without addition of $\text{ZrO}_2\text{-SiC}$ (synthesized via plasma route) have been fabricated. The base materials in these cases are white tabular alumina and white fused alumina. Physical, chemical, thermal, thermo-mechanical and pyro-chemical properties were evaluated and compared. The effects of base material on different properties were also evaluated. The effect of anti oxidants on thermo-mechanical properties were compared with the pyro-chemical properties done through simulative testing in rotary drum furnace. Also metal bonded plates were treated in nitrogen atmosphere at $> 1600^\circ\text{C}$ to synthesize nitride/oxy-nitride/sialon bonding and its impact on thermo-mechanical properties.

Chapter 4
Experimental

The raw materials used for manufacturing Al_2O_3 –C refractories were tabular alumina, white fused alumina, silicon metal powder, aluminium metal powder, carbon black, graphite flake and resin. For preparation of Al_2O_3 –C refractories, about 92-95 wt% alumina and remaining is metals and carbon. Resin was also used as Novalac resin (liquid resin), solid resin and hexamine.

4.1 Specification of raw materials

Table.4.1 Specification of raw materials for Al_2O_3 refractory

Raw materials (wt %)	TA	WFA	Al metal	Si metal	Carbon black	Graphite flake
Al_2O_3	99.5	99.3	-	-	-	-
Fe_2O_3	0.05	0.1	-	0.5	-	-
Si	-	-	-	97	-	-
Al	-	-	97.5	-	-	-
Carbon	-	-	-	-	99.5	97

4.2 Fabrication of Al_2O_3 based slide plates.

Optimum quantity of different grading were taken in a counter current mixture and mixed properly with the addition of liquid resin, solid resin and hexamine. Hexamine is used as a polymerising agent.

4.2.1 Batch preparation

Initially batches were prepared to form Al_2O_3 slide plates without carbon. Target was to optimise the metal addition for better thermo mechanical properties. Aluminium and Silicon metal in different combination was used in tabular and white fused alumina. Then carbon bonded batches were prepared using Carbon Black and Graphite Flake in various combinations. In the case of samples with ZrO_2 -SiC addition, the same method is followed. 20kg batches were prepared. So batch calculation of the raw materials had been done according to that. Raw materials are batched as fine, medium and coarse. The different compositions for batching are given in the tables 2, 3 and 4.

Table 4.2 Different recipes of Al₂O₃ refractory for slide plates. [TA stands for tabular alumina and WFA stands for white fused alumina]

Raw material	Trial -1 (wt%)	Trial -2 (wt%)	Trial -3 (wt%)	Trial -4 (wt%)	Trial -5 (wt%)
TA: mesh 8-14	25%	25%	Nil	Nil	25%
TA: mesh 14-28	10%	10%	Nil	Nil	10%
TA: mesh 28-48	20%	20%	Nil	Nil	20%
TA: -48 mesh	7%	10%	Nil	Nil	10%
TA: -325 mesh	20%	20%	20%	20%	20%
TA: -635 mesh	10%	10%	10%	10%	10%
WFA: (1-2)mm	Nil	Nil	25%	25%	Nil
WFA: (0-1)mm	Nil	Nil	37%	40%	Nil
Si metal (-325mesh)	3%	Nil	3%	Nil	5%
Al metal (-200mesh)	5%	5%	5%	5%	Nil
Novalak Resin (liquid)	3 parts	3 parts	3 parts	3 parts	3 parts
Resin solid	2.5 parts	2.5 parts	2.5 parts	2.5 parts	2.5 parts
Hexamine	0.3 parts	0.3 parts	0.3 parts	0.3 parts	0.3 parts

Table 4.3 Different recipes of Al₂O₃ - C refractory for slide plates. [TA stands for tabular alumina and WFA stands for white fused alumina]

Raw material	Trial -6 (wt%)	Trial -7 (wt%)	Trial -8 (wt%)	Trial -9 (wt%)
WFA: (1-2)mm	27%	25%	25%	25%
WFA: (0-1) mm	37%	37%	37%	40%
TA: -325 mesh	15%	20%	20%	20%
TA: -635 mesh	10%	10%	10%	10%
Carbon black	3%	1.50%	5%	2.50%
Graphite flake	Nil	1.50%	Nil	2.50%
Si metal (-325mesh)	3%	3%	3%	3%
Al metal (-200mesh)	5%	5%	5%	5%
Novalak Resin (liquid)	3 part	3 part	3 part	3 part
Resin solid	2.5	2.5	2.5	2.5
Hexamine	0.3	0.3	0.3	0.3

Al₂O₃ -C refractories are having oxidation problem and have to improve thermo-mechanical properties. To improve Thermal Shock Resistance, corrosion resistance and oxidation resistance, along with mechanical properties batches were prepared with addition of ZrO₂-SiC in Al₂O₃-C. ZrO₂-SiC of (-325) mesh size was used. Sieve analysis had been done for confirming the required size.

Table 4.4 Different recipes of Al_2O_3 – C - ZrO_2 - SiC refractory for slide plates. [TA stands for tabular alumina and WFA stands for white fused alumina]

Raw material	Trial-10 (wt%)	Trial -11 (wt%)	Trial-12 (wt%)	Trial -13 (wt%)
WFA: (1-2)mm	25%	25%	25%	25%
WFA: (0-1) mm	37%	37%	37%	37%
TA: -325 mesh	20%	20%	20%	20%
TA: -635 mesh	10%	10%	10%	10%
Carbon black	1.5%	1.50%	1.5%	1.50%
Graphite flake	1.5%	1.50%	1.5%	1.50%
Si metal (-325mesh)	3%	3%	3%	3%
Al metal (-200mesh)	5%	5%	5%	5%
Novalak Resin (liquid)	3 part	3 part	3 part	3 part
Resin solid	2.5	2.5	2.5	2.5
Hexamine	0.3	0.3	0.3	0.3
ZrO_2 - SiC	Nil	0.5	1	1.5

4.2.2 Mixing

After batching, the raw materials are mixed in Eirich mixer/counter current mixer. Coarse and medium materials are added first and dry mixing has been done for 5 minutes. Then liquid resin (Novalak resin) was added and wet mixing continued for next 5 minutes. For carbon containing samples carbon would be added next. In other case metals are added and mixed for 5 minutes. Then fine material addition and mixing for 15 minutes. The solid resin and hexamine are added in the end. Hand pressing was done to check the consistency of the mixture.

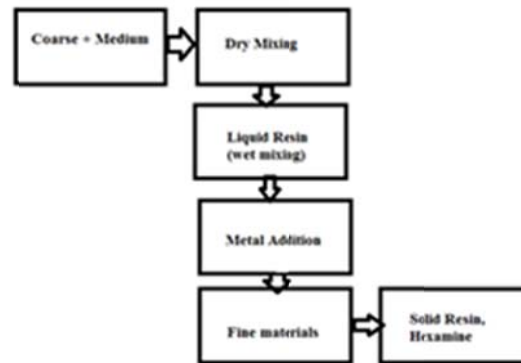


Fig 4.1 Mixing sequence for Al_2O_3 based refractory

4.2.3 Ageing

Mixed samples were kept in a controlled temperature chamber for ageing for 24 hours. Purpose of ageing is volatile material removal. After crushing and properly screening, volatile material is checked.

4.2.4 Pressing

After ageing, the mixture was filled in a mould and were pressed to slide plates in hydraulic press at 400 Ton with a specific pressure of 2000kg/cm².. While filling the mould uniform filling is required to get homogeneity. Pressing is done to give shape to the aggregate, and for getting good density with less porosity. After pressing the slide plates were taken for drying.

4.2.5 Tempering

Sample was cured at 240 °C for 12 hours. It is for removing moisture and also for attaining green strength for the bricks. At this stage liquid resin gets converted to carbonaceous phase and the strength of bonding increased.

4.2.6 Coking

The dried samples are fired at 1100 °C for 6 hrs inside a bell kiln. The atmosphere inside the furnace was reducing.

4.3 General characterisation of Al₂O₃ refractory

4.3.1 Physical properties

4.3.1.1 Apparent porosity and Bulk density

Definition of apparent porosity can be given as volume of open pores to the total volume of sample (bulk volume). $Apparent\ porosity = \frac{Total\ Volume\ of\ open\ pores}{Total\ volume\ of\ the\ sample}$

According to ASTM C-20 bulk density (BD) and apparent porosity (AP) are determined. For measuring the apparent porosity and bulk density of fired samples Archimedeian evacuation method was followed, and water was used as the medium. Sample was cut into 30×30×40 mm size for AP/BD measurement. Dry weight of the sample was noted initially. Keeping sample in a desiccator and after creating vacuum in it, water was introduced to soak the sample. Then suspended weight of sample was taken by suspending it in water. After removing the surface water with a wet cloth soaked weight of sample was taken.

Dry weight of sample = D gm, suspended weight of sample = S gm, soaked weight of sample = W gm. From the above weights, apparent porosity of the samples are calculated as $AP(\%) = \left(\frac{W-D}{W-S} \right) \times 100$

Bulk density is the ratio of mass of a dry sample to its bulk volume. Bulk volume = volume of solid material + volume of closed pores. From the above weights the bulk density of the samples are calculated as BD (gm/cc) $= \frac{D}{W-S} \times density\ of\ liquid\ in\ that\ temperature.$

4.3.1.2 Cold crushing strength

Cold crushing strength of a refractory is the gross compressive stress required to cause failure. It gives idea about the bonding strength and strength of grains. The measuring standard for Cold crushing strength for refractory specimen is ASTM C-133. The bricks are cut in the desired dimension 25×25×25mm. The sample is kept on flat surface, in between bedding material, in the testing machine as shown in the fig 4.2. Uniform load is applied on the flat surface of the specimen with the mechanical compression testing machine. The load at which crack started appearing is considered as cold crushing strength of the specimen. The formula for calculating CCS is

$$\frac{\text{Load}}{\text{Area}} \text{ kg/cm}^2$$

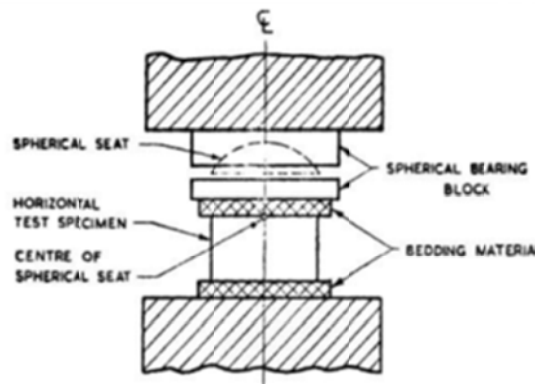


Fig 4.2 Schematic representation of compressive testing setup.

4.3.2 Mechanical and thermo-mechanical properties

4.3.2.1 Modulus of rupture and hot modulus of rupture

Modulus of rupture /cold modulus of rupture gives the flexural strength of refractory material at room temperature. It gives the maximum load carrying capacity of a member in bending. Three point bending test is used for finding the MOR of the specimen. The standard dimension will be 150×25×25mm and the span length is usually 125mm. The unit of MOR is kg/cm^2 .

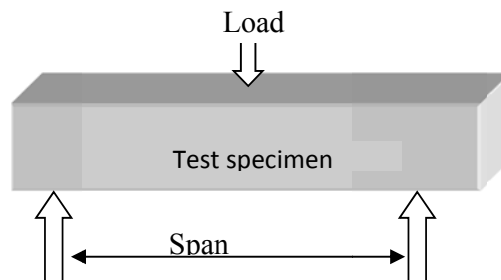


Fig 4.3 Schematic representation of 3 point bending test

Hot modulus of rupture is the same as cold modulus of rupture but at elevated temperature. It is measured according to the standard ASTM C 133-7 with HOT MOR TESTER, BYSAKH & CO apparatus. The specimen was kept in the apparatus in the specified position. It was fired at 1400 °C with 30 minutes dwelling time. It was done in air atmosphere with 5°C/min heating rate. Then it was subjected to 3 point bending.

The formula for calculating HMOR is $(3PL)/(2bd^2)$, unit of HMOR is kg/cm²

P = maximum load(kg) at which the specimen breaks.

L = span length (mm), b = breadth of the specimen (mm).

d = depth of the specimen (mm)

4.3.3 Thermal and Thermo-chemical properties

4.3.3.1 Thermal shock resistance

When refractory materials were subjected to rapid temperature change, thermal stresses developed in it. Resistance to fracture because of these conditions are termed as thermal shock resistance or thermal spalling resistance [8]. Heating the material in high temperature and sudden cooling by bringing into ambient conditions is the standard method for evaluating thermal shock resistance. It is measured according to the standard ASTM C 1171. Before the test, the sample was coated with high temperature coating material. The sample was heated to 1200°C for 30 minutes and quickly brought to ambient conditions, kept for 10 minutes. It was repeated. The number of cycles required for failure under such rapid temperature changes gives the thermal spalling resistance.

4.3.3.2 Erosion resistance

Rotary slag test is done for evaluating erosion resistance of the sample. It was done in rotary drum instrument. The standard used for testing was ASTM C-874. Sample dimension used was 160×30×40mm. The samples were given coating of high temperature coating material. Inside the sample holder the samples were lined with the help of mortar. After drying, this drum was fitted to the rotary drum apparatus. Gas cylinders were being connected to apparatus. 5 rotations per minute was the speed of the rotary drum. The samples were undergone preheating for 1 hour at 1000 °C. Then through the holes/openings in the sample holder, small amount of metal (iron rod) was added. Then small amount of LD slag was added in the sample holder. The 1550°C temperature was maintained for 1 hour. Metal and slag were tapped out and fresh ones

were replaced. This tapping repeated for 2 times and stopped. The samples are taken out and evaluated by measuring the depth of erosion in the samples.

4.3.3.3 Oxidation resistance

For finding the oxidation resistance the sample was cut in the dimension 30×40×40mm. It was fired in the furnace at 1400°C for 2 hours in air atmosphere. The oxidation of the brick was evidently seen by the colour of the oxidised portion of brick. The area of the oxidised portion was measured.

$$Oxidation(\%) = \frac{Area\ of\ oxidised\ zone}{Total\ area} \times 100$$

4.3.4 Phase Analysis by X-ray diffraction

The phase analysis study of the samples were carried out in XRD instrument [PANalytical, X'pert Pro] using Cu K_α. The diffraction patterns which were obtained from the instrument were analysed using Xpert Highscore software.

4.3.5 Micro structural Analysis

4.3.5.1 Optical microscopy/ SEM/FESEM/EDS

After polishing the sample by paper polishing, cloth polishing and then by diamond paste, the surface images were taken using optical microscope(ZEISS,AXIO SCOPE.A1).Initial study of the microstructure were made using the optical microscopy images. The topography and grain morphology of the samples were studied using scanning electron microscopy (Joel/eo) .It uses a beam of highly energetic electrons to examine objects on a very fine scale. Composition and crystallographic information were also obtained from SEM. A more detailed study of the microstructure of the samples were done using Field emission scanning electron microscopy (Nova NanoSEM 450). And the elemental analysis of the compositions was made possible by Energy dispersive X-ray spectroscopy (EDS).

Chapter-5
Results and Discussion

5.1 Metal bonded Al_2O_3 slide plate

5.1.1 Physical properties

Figure 5.1 (a), (b) and (c) shows the AP, BD and CCS of tempered and coked samples of composition T-1, T-2, T-3, T-4 and T-5, respectively.

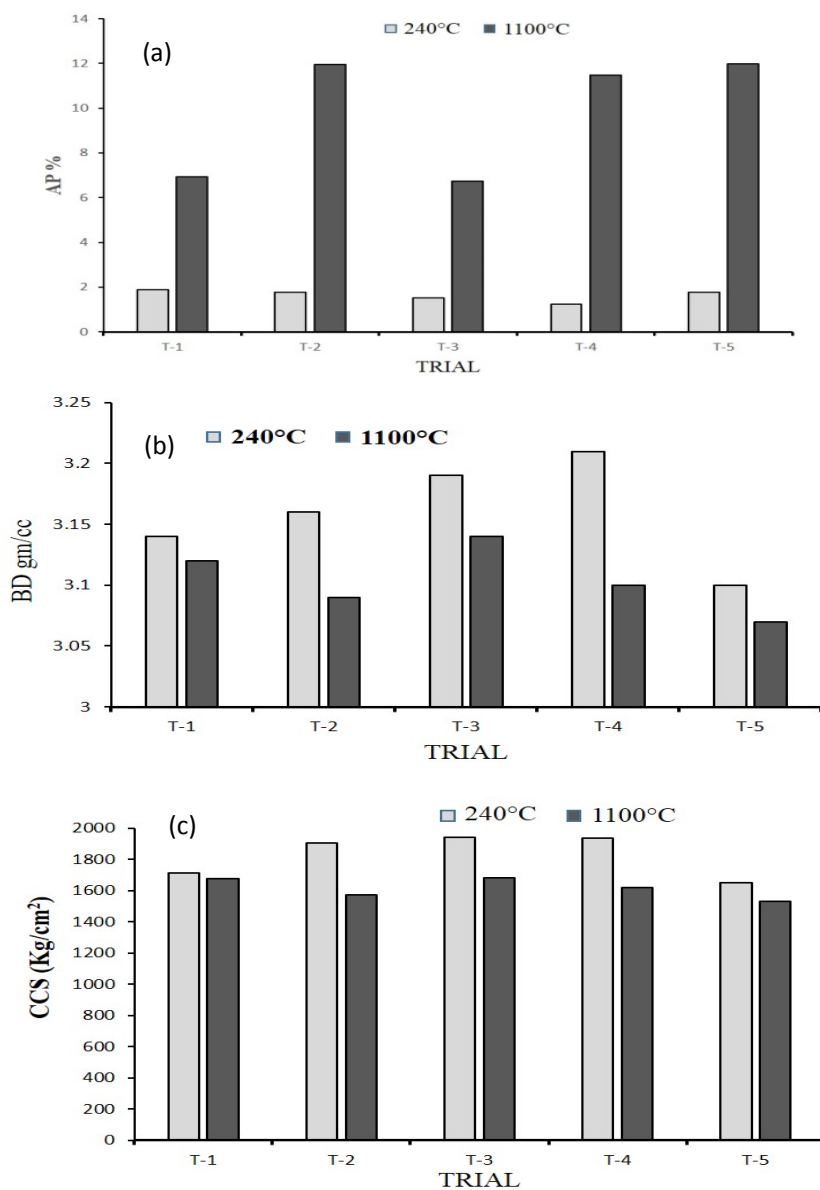


Fig.5.1: Variation of AP (a), BD (b) and CCS (c) of different tempered and coked samples

Considering the physical properties like AP, BD and CCS, the composition T-3 was showing better results especially after coking. From the graph, it was observed that at drying state apparent porosity was very low and after firing apparent porosity increased. This was due to the removal of volatile matter during firing. In the case of apparent porosity, sample T-3 was having 6.75% which was the best result for AP, whereas T-1 was having AP as 6.93%. So the samples with metals in combination were having good results for apparent porosity. In the case of bulk density the maximum bulk density was seen in sample T-3 with 3.12 gm/cc. The sample T-5 which was having only silicon metal was having the lowest value of 3.07 gm/cc. Cold crushing strength of the samples were excellent, 1682.98 kg/cm² was the highest CCS after coking and it was seen in sample T-3. So the samples containing white fused alumina was showing better properties. Samples containing metal in combination was having the upper hand for AP, BD and CCS. White fused alumina samples were showing better physical properties as compared with tabular alumina samples, due to higher crystal size and grain bulk density resulting in improved packing density of white fused alumina. Also it was shown that the samples containing only Al metal showed better AP, BD and CCS than only Si metal containing samples. This is because the formation of carbide is much easier in aluminium compared to silicon.

5.1.2 Mechanical and thermo-mechanical properties

5.1.2.1 Modulus of rupture, hot modulus of rupture

Figure 5.2 and 5.3 shows MOR and HMOR of tempered and coked samples of composition T-1, T-2, T-3, T-4 and T-5, respectively. For the mechanical and thermo mechanical properties like MOR and HMOR, sample T-3 was showing better results. It was found that white fused alumina with 3% Si and 5% Al was the best among all the above compositions. Excellent HMOR value of 217.86 kg/cm² was observed in sample T-3 and 205.02 kg/cm² for sample T-1, after coking. This is due to the presence of both the metals as the combination of silicon and aluminium lead to the formation of aluminium silicon carbide (Al₄SiC₄) [as confirmed from XRD], which effectively improved the mechanical strength of the composition. Here, carbon was present in the sample by the use of phenolic resin. At high temperature it provides carbonaceous bond, and also the firing had taken place in coke atmosphere, which made the favourable conditions for carbide formation. It was also confirmed that the sample containing Al are better in both mechanical and thermo mechanical properties point of view as

compared with with Si containing samples. The formation of Al_4C_3 [as confirmed from XRD] in the Al containing samples is the reason for the strength at high temperature ^[4]. However, SiC was not observed in XRD for Si containing samples. As, the carbide formation in silicon containing sample is not easy, compared with aluminium containing samples.

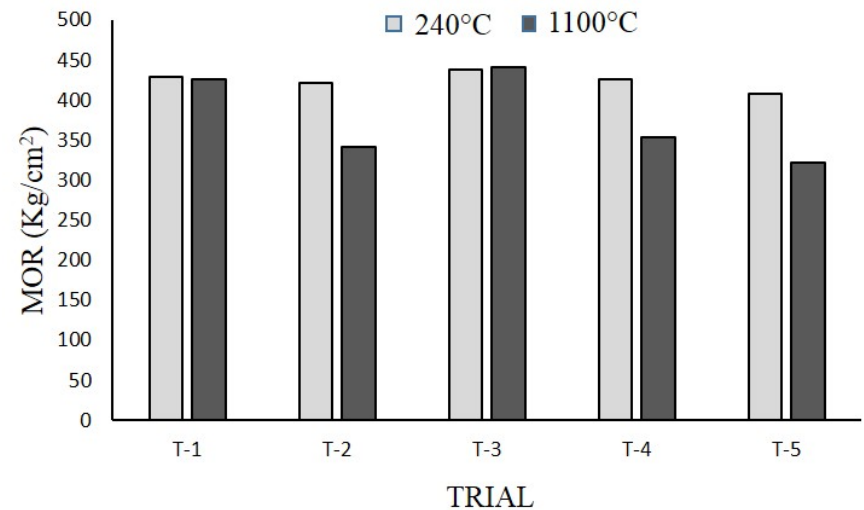


Fig.5.2 Variation of MOR for the samples cured at 240 °C and fired at 1100 °C for 6h in coke environment.

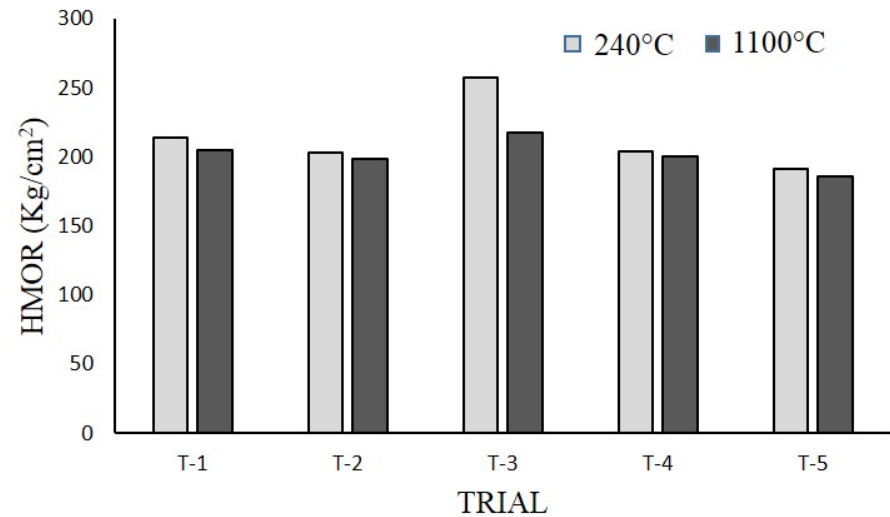


Fig.5.3 Variation of HMOR for the samples cured at 240 °C and fired at 1100 °C for 6h in coke environment.

5.1.3 Structural properties

Figure 5.4 shows the XRD patterns of Al_2O_3 samples of compositions T-1, T-2, T-3, T-4 and T-5 tempered at 240 °C and coked at 1100 °C.

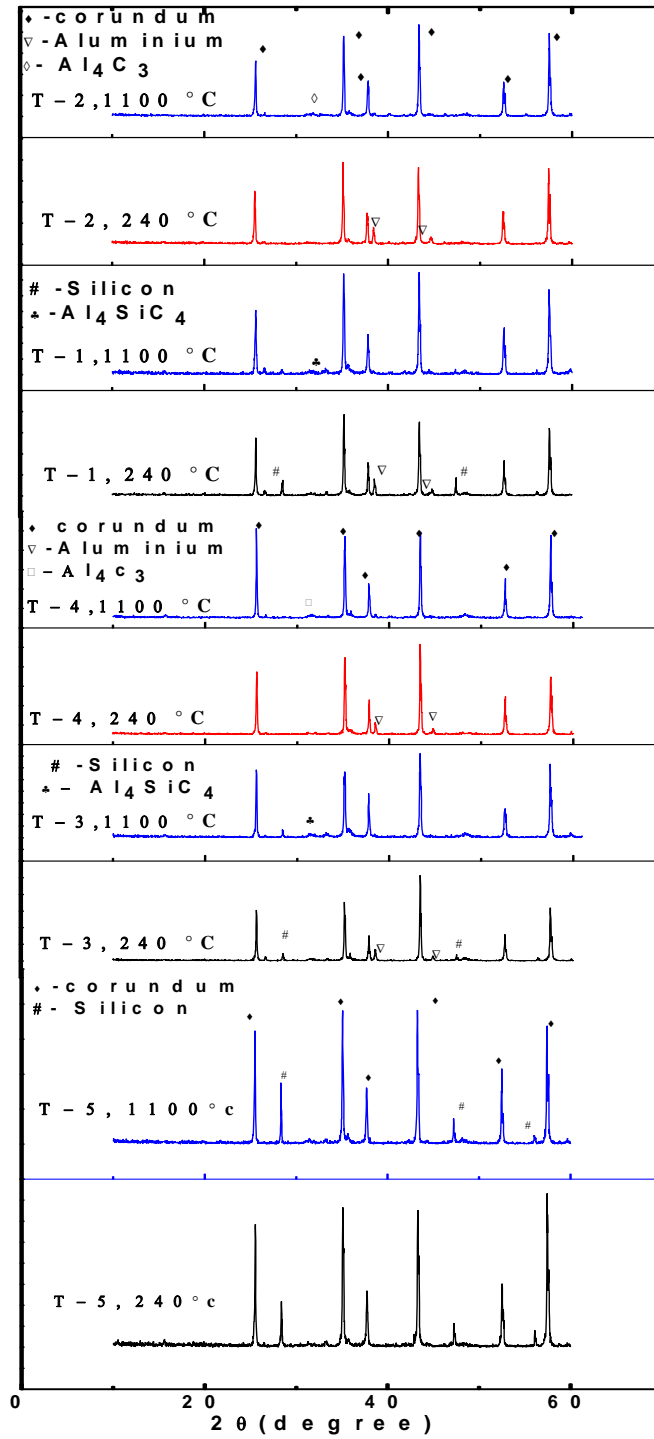


Fig. 5.4 XRD patterns of Al_2O_3 samples tempered at 240 °C and coked at 1100 °C.

From the XRD analysis, it is clear that the major peaks in all the samples are of corundum. In samples of composition T-1, T-2, T-3 and T-4, the peaks of metal are visible in the dry state, but after coking, the peak intensity of the metal reduced drastically. This was due to the formation of carbide. For samples T-1 and T-3, formation of aluminium silicon carbide (Al_4SiC_4) was identified from the XRD graphs. Also Al_4C_3 was formed in a similar manner in the samples T-2 and T-4. However, after coking, the peak intensity of metal (Si) of sample T-5 was not reduced as drastically as other samples mentioned above. So, silicon containing samples were not showing good results in terms of physical as well as mechanical properties as compared with aluminium containing samples.

5.1.4 Micro structural properties

5.1.4.1 FESEM, EDS and optical microscopy

Fig 5.5 (a) and (b) shows the optical image of sample T-3, before and after coking, respectively.

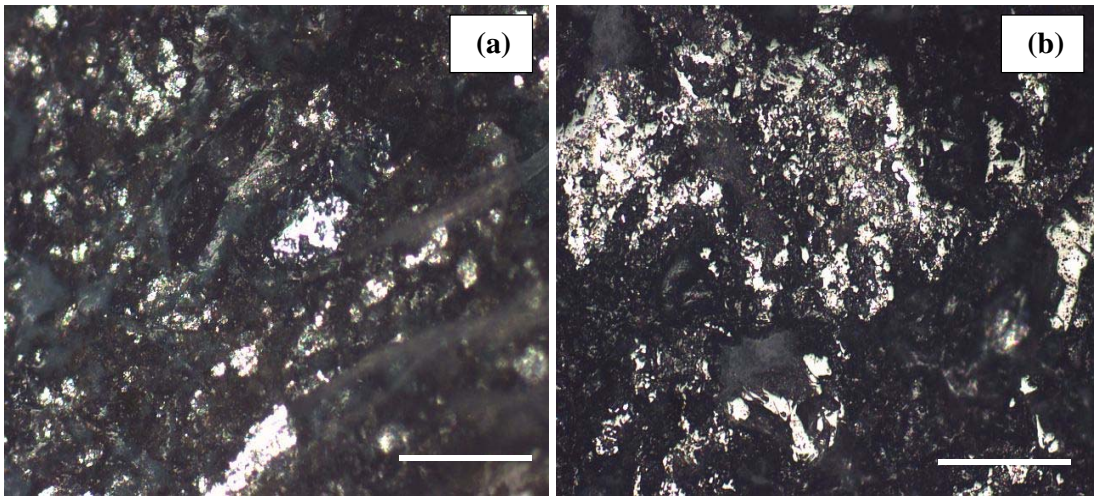


Fig 5.5: Optical image of sample T-3, (a) before and (b) after coking.

In the optical micrograph of Fig. 5.5 (a), the presence of aluminium and silicon metal was observed (brighter portion) at tempered state. After coking, the formation of carbide was observed (brighter portion) as seen in the Fig 5.5 (b). For detailed information about the microstructure, FESEM with EDS of the sample was performed.

Fig 5.6 (a) and (b) shows the FESEM micrographs of sample T- 3 at tempered and coked state, respectively. Fig 5.6 (c) shows the EDS analysis of sample T- 3 at coked state.

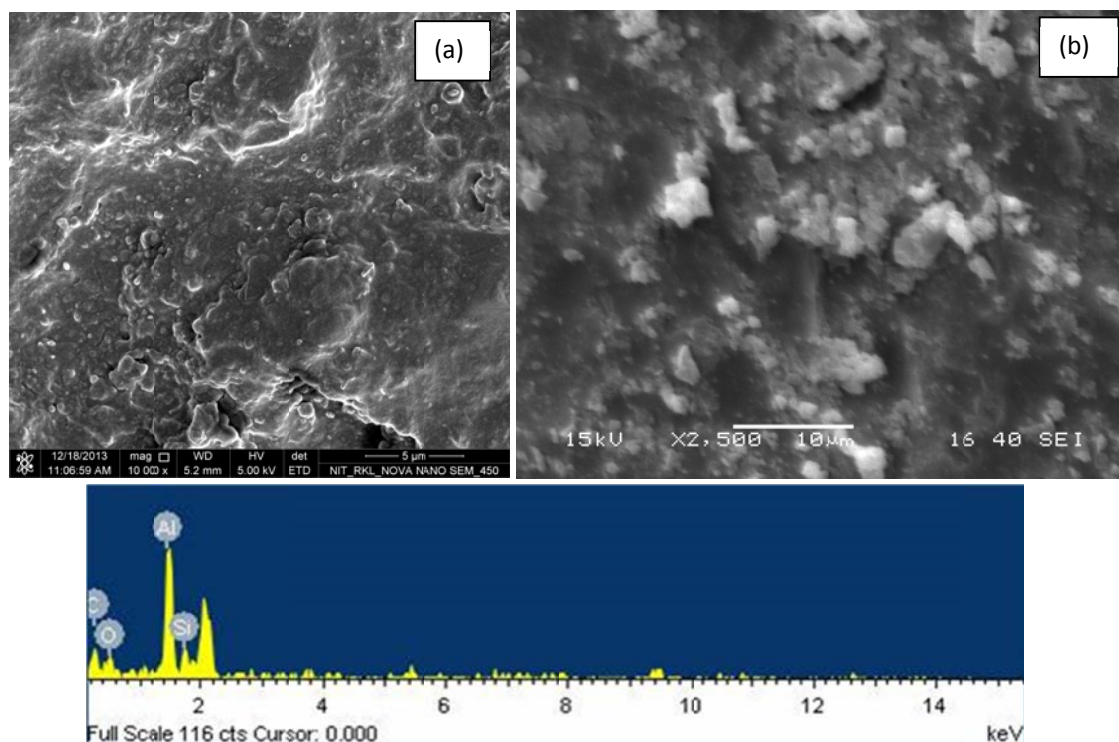


Fig 5.6 FESEM micrograph of sample T- 3 at tempered state (a); SEM micrograph of sample T- 3 at coked state (b) and EDS analysis of sample T- 3 at coked state (c).

The brighter contrast in image of Fig. 5.6 (a) indicates the presence of the metals either aluminium or silicon. In Fig 5.6 (b) carbide formation was observed, which was confirmed by the EDS analysis of this sample. This carbide is aluminium silicon carbide (Al_4SiC_4), as it was confirmed from XRD analysis.

To further understand the morphology of other samples such as T-1, T-2, T-4 and T-5 in the coked state, FESEM/SEM micrographs were performed on these samples. Fig 5.7 (a), (b), (c) and (d) shows the SEM/FESEM micrographs of coked samples T-1, T-2, T-4 and T-5, respectively. Similar kind of carbide formations is visible (brighter contrast) in the samples T-1, T-2 and T-4 after coking. The carbide formation was Al_4SiC_4 in T-1 and Al_4C_3 in T-2 and T-4, as confirmed from XRD analysis. However, only silicon metal containing sample in T-5, the carbide formation was not so much observed after coking [no such brighter contrast was observed in Fig. 5.7 (d)].

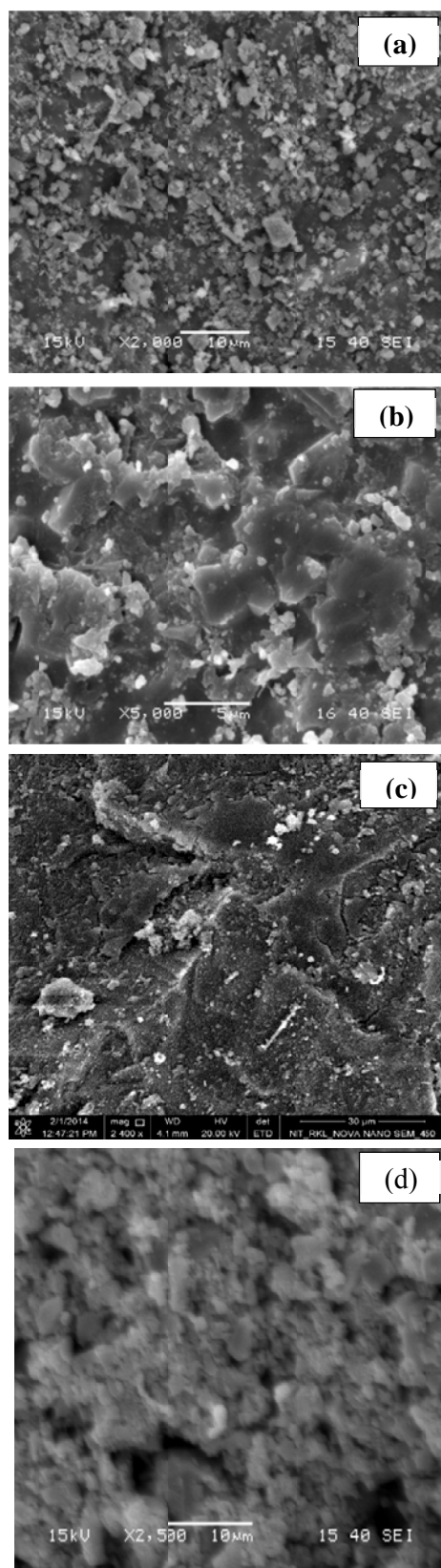


Fig 5.7 FESEM micrograph of coked sample: (a) T-1, (b) T- 2, (c) T-4 and (d) T-5.

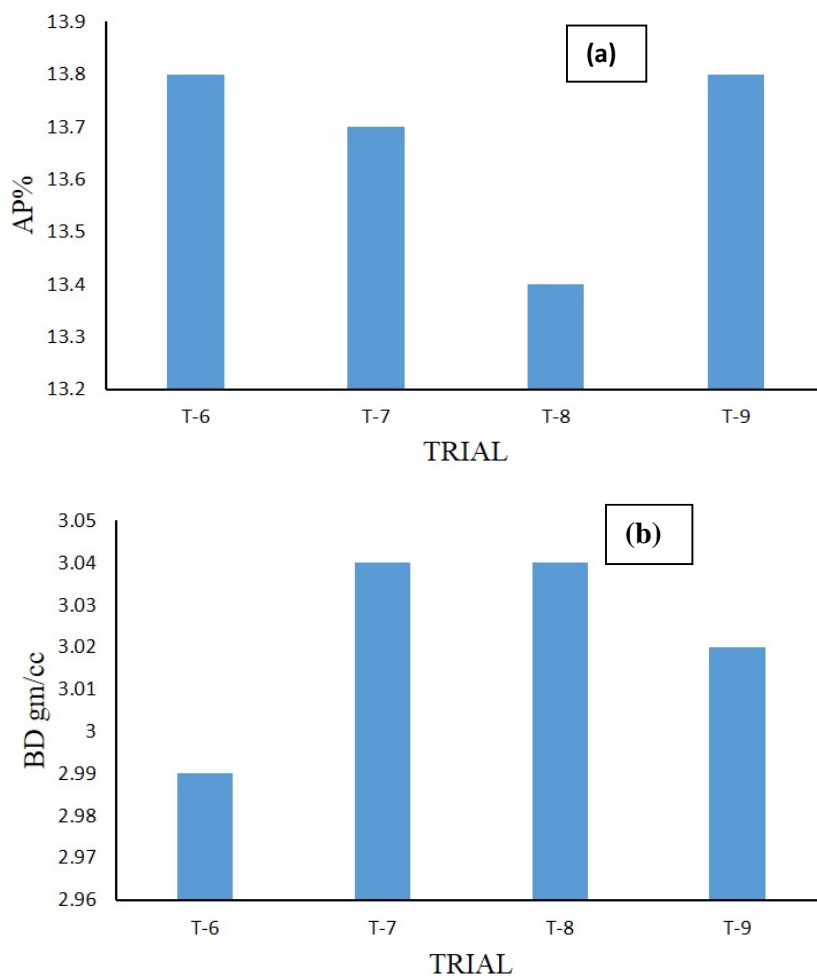
5.2 Carbon bonded Al_2O_3 Slide plate ($\text{Al}_2\text{O}_3\text{-C}$)

The optimum composition from metal bonded samples was further utilized for fabrication of $\text{Al}_2\text{O}_3\text{-C}$ refractories. From the metal bonded samples, the optimum composition was white fused alumina with combination of metals (Al + Si). To fabricate $\text{Al}_2\text{O}_3\text{-C}$ refractories, different types as well as concentration of carbon have been added to the optimized composition in metal bonded Al_2O_3 . Further, effect of carbon on physical, thermal and thermo-mechanical properties of $\text{Al}_2\text{O}_3\text{-C}$ refractories have been studied and analyzed.

5.2.1 Physical properties

5.2.1.1 Apparent porosity, bulk density and cold crushing strength

Fig 5.8 (a), (b) and (c) shows the variation of apparent porosity, bulk density and cold crushing strength of the samples T-6, T-7, T-8 and T-9, respectively.



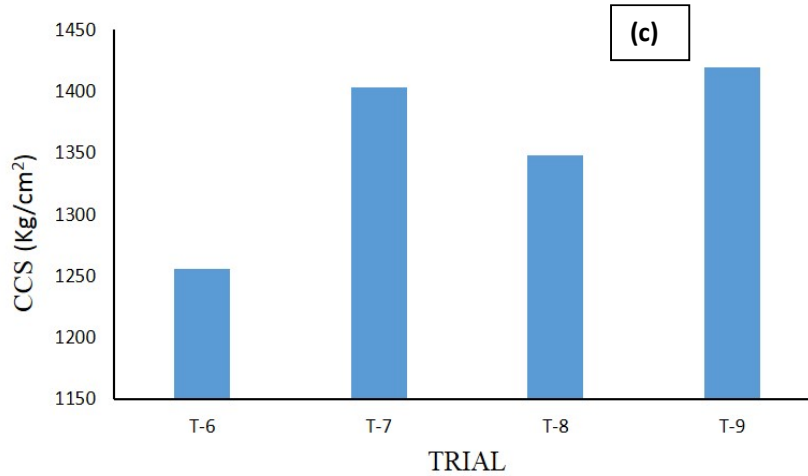


Fig.5.8 Variation of (a) apparent porosity, (b) bulk density and (c) CCS of carbon bonded samples.

Different carbon sources in different proportion are used in the trials T-6, T-7, T-8 and T-9. Comparing with metal bonded samples, the value of apparent porosity in carbon bonded samples increased to 13 %. Similarly, bulk density was also decreased when compared with metal bonded samples. Maximum value of BD was ~ 3.04 g/cc in white fused alumina based carbon bonded samples. However, the CCS value of this carbon bonded seems interesting. T-6 and T-7 are low carbon containing samples and T-8 and T-9 are high carbon samples. Sample T-7 (low carbon with graphite flake) and T-9 (high carbon with graphite flake) shows better CCS results, as compared to sample T-6 and T-8. Higher CCS value of graphite flake containing samples may be due to sliding mechanism within graphite layers in the matrix.

5.2.2 Mechanical and Thermo mechanical properties

5.2.2.1 Modulus of Rupture and Hot modulus of rupture

Fig. 5.9 (a) and (b) shows MOR and HMOR of carbon bonded samples (T-6, T-7, T-8 and T-9), respectively. The composition, in which both carbon black and graphite flake were used, shows good MOR as well as HMOR. The maximum MOR and HMOR value was 292.84 kg/cm^2 and 131 kg/cm^2 , respectively for sample T-7. The presence of graphite flakes enhances the mechanical strength. This is mainly due to sliding mechanism, which is operating between graphite layers helped to enhance the mechanical strength ^[12, 31]. Comparing with high carbon samples T-8 and T-9, the low

carbon samples T-6 and T-7 were showing better mechanical strength. This is due to the fact that when carbon content increases mechanical strength decreases.

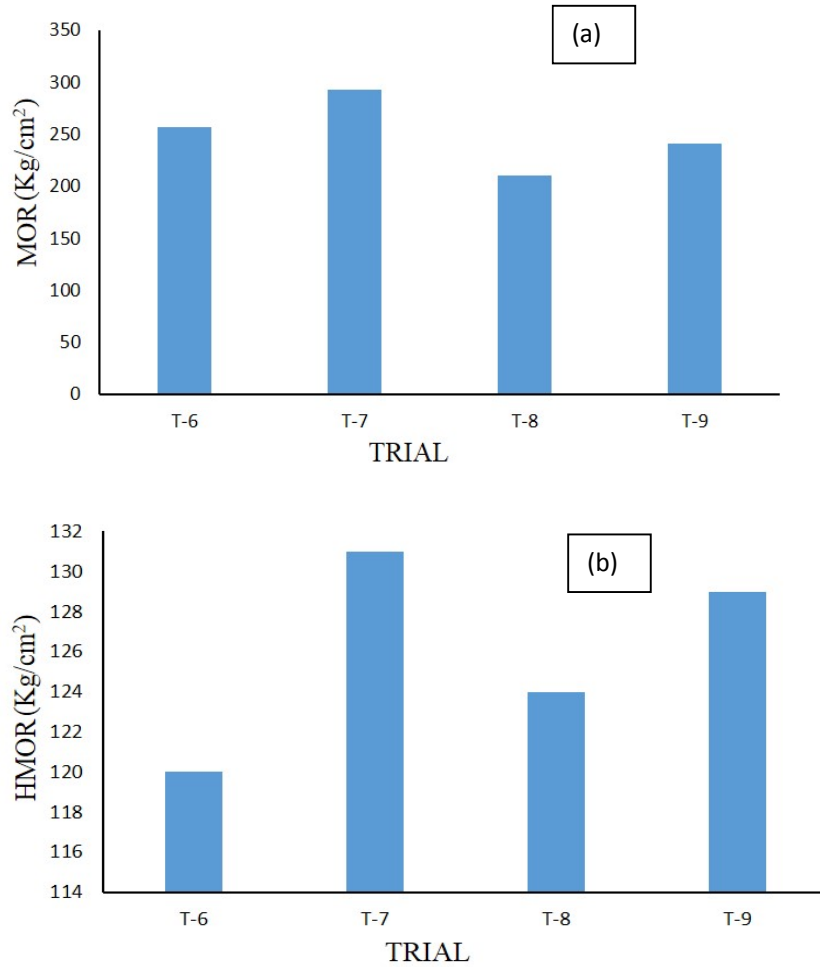


Fig. 5.9 Variation in (a) MOR and (b) HMOR of carbon bonded samples.

5.2.3 Microstructure

Fig 5.10 (a), (b), (c) and (d) shows the FESEM micrographs of coked samples T-6, T-7, T-8 and T-9, respectively. Formation of whiskers or fiber like morphology was observed in all the samples. Samples containing graphite flakes lead to form concentrated fibers/whiskers as compared with carbon black samples [see Fig. 5.10 (c) and (d)]. The presence of these whiskers was the one of the main reason to enhance the properties of this refractory material. These whiskers might belong to aluminium silicon carbides.

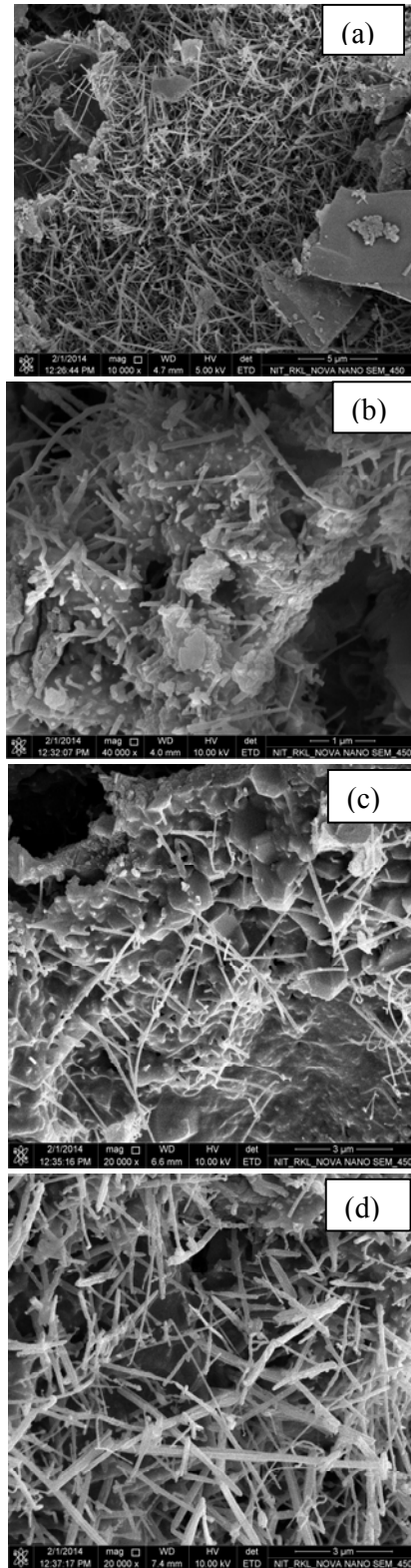


Fig. 5.10 FESEM micrographs of coked sample (a) T-6, (b) T-7, (c) T-8, and (d) T-9.

5.3 ZrO₂-SiC bonded Al₂O₃-C Slide plate.

In this section, different percentages of ZrO₂-SiC bonded Al₂O₃-C based refractories was studied and analyzed. ZrO₂-SiC was fabricated using plasma fusion method. This material was added in optimized Al₂O₃-C matrix (as mentioned above) having composition with white fused alumina and combination of both metals along with mixture of 1.5% carbon black and 1.5% graphite.

5.3.1 Physical properties

5.3.1.1 Apparent porosity, bulk density and cold crushing strength

Figure 5.11 (a), (b) and (c) shows AP, BD and CCS of coked samples (T-7) as a function of wt % of ZrO₂-SiC.

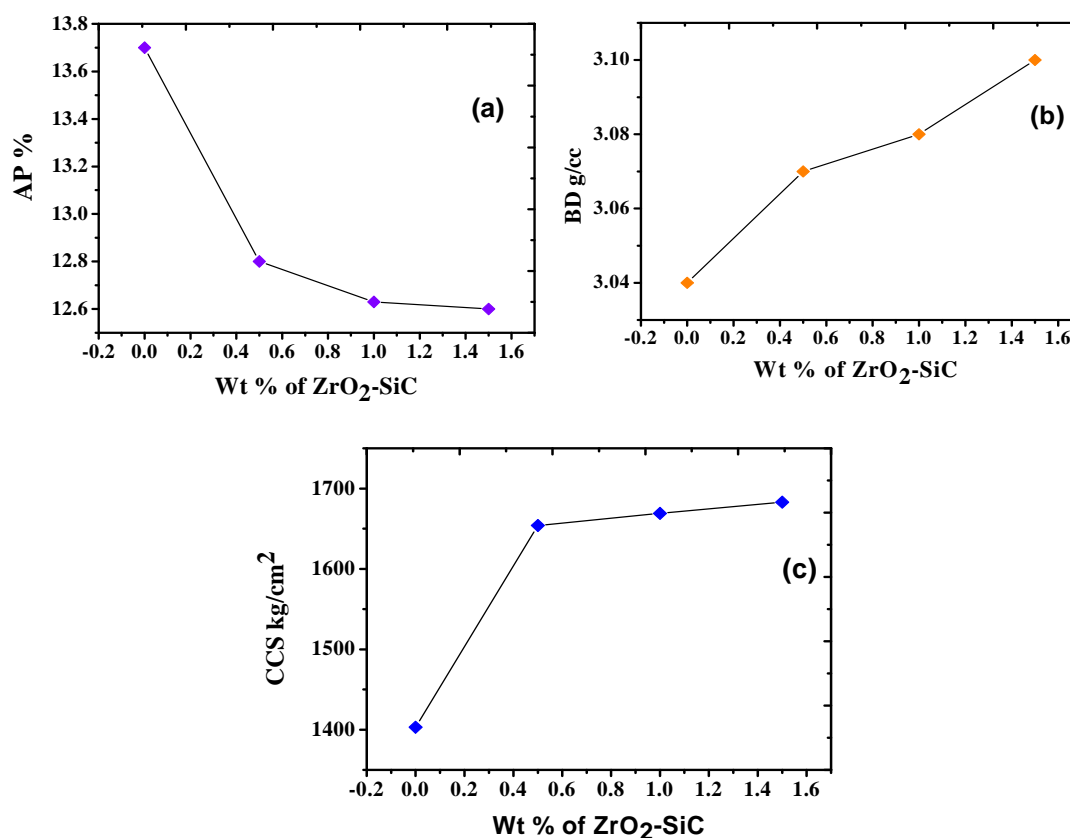


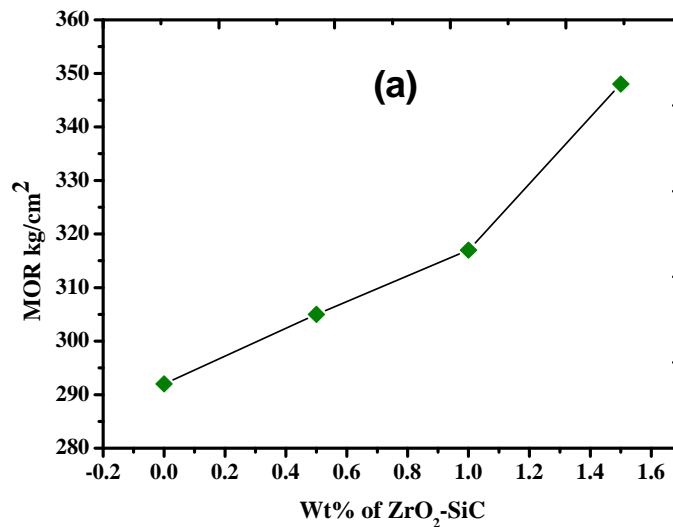
Fig.5.11 Variation in (a) AP (b) BD and (c) CCS of coked T-7 samples as a function of ZrO₂-SiC

From the graphs it was quite clear that AP, BD and CCS of the sample improved significantly with the addition of $\text{ZrO}_2\text{-SiC}$. The reason behind these improvements may be due to high toughness properties of ZrO_2 and SiC. The apparent porosity of the base composition was 13.7%. By the addition of 0.5% $\text{ZrO}_2\text{-SiC}$, it has been improved to 12.8% apparent porosity. The bulk density of the base composition was 3.04 gm/cc. It has been increased to 3.07 gm/cc by the addition of 0.5 % addition of $\text{ZrO}_2\text{-SiC}$, further increased to 3.08 and 3.10 gm/cc for 1% & 1.5% addition respectively. The addition of $\text{ZrO}_2\text{-SiC}$ improved the cold crushing strength of the material to a greater extent. The base composition CCS value was 1403 kg/cm^2 and it has been increased to values above 1600 Kg/cm^2 by $\text{ZrO}_2\text{-SiC}$ addition. The reason behind the improvement in physical properties is the strength and toughness provided by ZrO_2 and SiC and their influence on sintering. ZrO_2 addition works as an oxygen donor for the formation of oxy carbide bonding. Formation of more carbides were also enhancing the strength of the samples.

5.3.2 Mechanical & Thermo-mechanical properties

5.3.2.1 Modulus of rupture, hot modulus of rupture

Fig.5.12 (a) and (b) shows variation in modulus of rupture and hot modulus of rupture of $\text{Al}_2\text{O}_3\text{-C}$ samples with addition of $\text{ZrO}_2\text{-SiC}$.



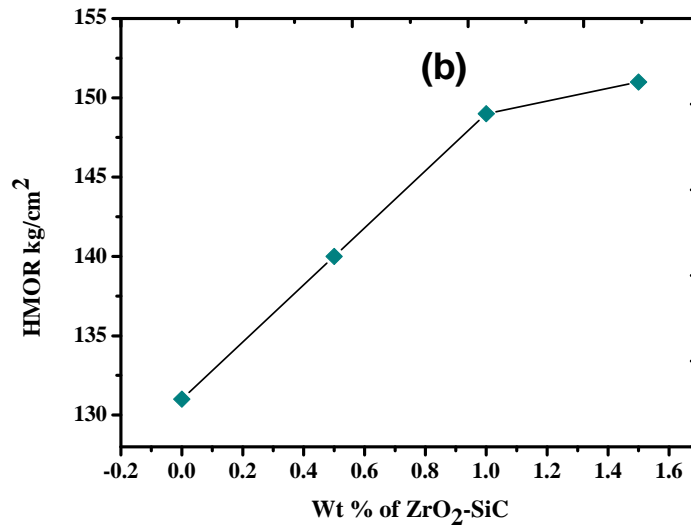


Fig.5.12 MOR (a) and HMOR (b) as a function of wt % ZrO₂-SiC in Al₂O₃-C

From the plot it was clear that ZrO₂-SiC addition has improved the mechanical strength significantly. MOR value of base composition was 292 Kg/cm² and it has been increased to a maximum of 348 kg/cm² by 1.5% addition of ZrO₂-SiC. The base composition of Al₂O₃ -C was having 131 kg/cm² as HMOR, and by adding 0.5% ZrO₂-SiC, it has been increased to 138 kg/cm². The strength and toughness provided by ZrO₂ and SiC were the reasons behind these results. SiC is acting as a seed for carbide formation. More SiC were formed and thus improves the properties to a higher level.

5.3.3 Oxidation Resistance

The samples [T10 (0), T-11 (0.5 wt% ZrO₂-SiC), T-12 (1 wt% ZrO₂-SiC), T-13(1.5 wt% ZrO₂-SiC)] are fired at 1400°C for 2 hours in air atmosphere. Oxidation of carbon took place in air atmosphere. The total area that has been oxidised was measured for each sample and the percentage of oxidation was calculated. Image of oxidation resistance of various samples was shown in Fig. 5. 13. From the images, it was confirmed that the oxidation resistance increases with the percentage of ZrO₂-SiC in Al₂O₃-C sample. Considering the initial sample (T-10) as having oxidation index 100, the relative oxidation index of the remaining samples was calculated. The lower the oxidation index, the better is the oxidation resistance of the sample. Figure 5.14 shows

the variation in oxidation index with respect to addition of $\text{ZrO}_2\text{-SiC}$. From the graph it was quite clear that the oxidation index decreases with increase in $\text{ZrO}_2\text{-SiC}$ percentage. This result indicates the resistance to oxidation increases. Oxidation resistance has significantly improved by addition of $\text{ZrO}_2\text{-SiC}$, because of more carbide formation. In this sample SiC was acting as a seed for carbide formation. The quantity of carbide formation would decide the oxidation. In this sample, more number of SiC were formed and the more the formation of carbides the lesser would be the chance of oxidation.

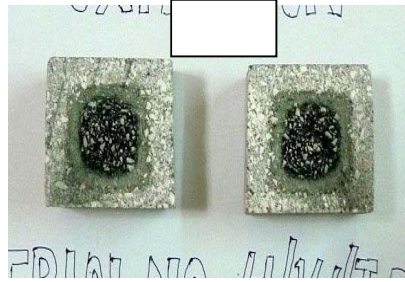


Fig. 5.13 Images of oxidation resistance of $\text{ZrO}_2\text{-SiC}$ added $\text{Al}_2\text{O}_3\text{-C}$ samples.

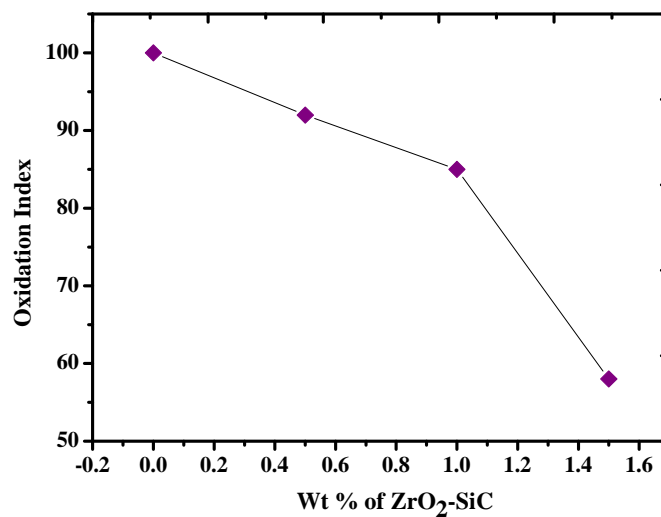


Fig.5.14 Oxidation index as a function of wt % of $\text{ZrO}_2\text{-SiC}$ in $\text{Al}_2\text{O}_3\text{-C}$ sample.

5.3.4 Thermal Shock resistance

The base composition sample T-10 broke into 2 pieces in 33rd thermal cycle. Sample T-11, T-12 and T-13 showed significant improvement by withstanding up to 100 thermal cycles. The thermal spalling resistance was improved significantly by the addition of ZrO₂-SiC mainly because of the presence of SiC.

5.3.5 Erosion Resistance

The rotary drum test was carried out to evaluate erosion resistance of the samples. In this pyro-chemical test samples were evaluated with respect to their oxidation, abrasion, corrosion and erosion creating the simulative condition as in an actual ladle in a rotary furnace after lining 10 numbers of samples. Thickness of the sample was around 40mm. The furnace was fed with mild steel and ladle slag having C/S ratio 2.5, Al₂O₃ content was maintained at 10%, MgO 5% and Fe₂O₃ was 3.5 %. Total operation time was 5 hours. After 30 minutes metal and slag was renewed. The result from the slag rotary test revealed that the addition of ZrO₂-SiC in Al₂O₃-C refractories substantially improved the erosion resistance of the refractory. Fig. 5.15 shows the image of erosion of different ZrO₂-SiC added Al₂O₃-C samples.

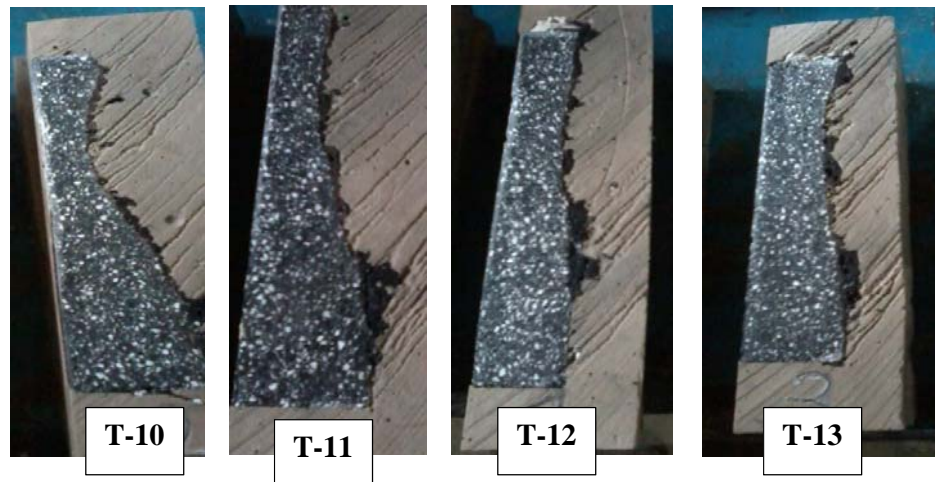


Fig.5.15 Variation in Erosion resistance by addition of ZrO₂-SiC in Al₂O₃-C sample.

Table-5.1 Variation in Erosion depth and Erosion index by addition of ZrO₂-SiC

Trial no	Original thickness in mm	Erosion in mm	Erosion index
10	40.2	22.27	100
11	40.3	16.86	75.7
12	40.1	10.9	48.94
14	40.1	10.67	48.4

From the Fig. 5.15, it was observed that as the percentage of $\text{ZrO}_2\text{-SiC}$ in the sample was increasing, the erosion depth was decreasing. From erosion depth values erosion index was calculated by keeping erosion index of base composition at 100. Variation in erosion index by $\text{ZrO}_2\text{-SiC}$ addition is shown in Fig 5.16. The detailed values are provided in Table 5.1. Lower the erosion index, higher the resistance to erosion. From the graph it was concluded that erosion resistance increases as the percentage of $\text{ZrO}_2\text{-SiC}$ addition increases. Here the non-wetting property of ZrO_2 was playing the major role. It will reduce the contact between the liquid slag and the refractory sample, thereby reducing the chance of erosion.

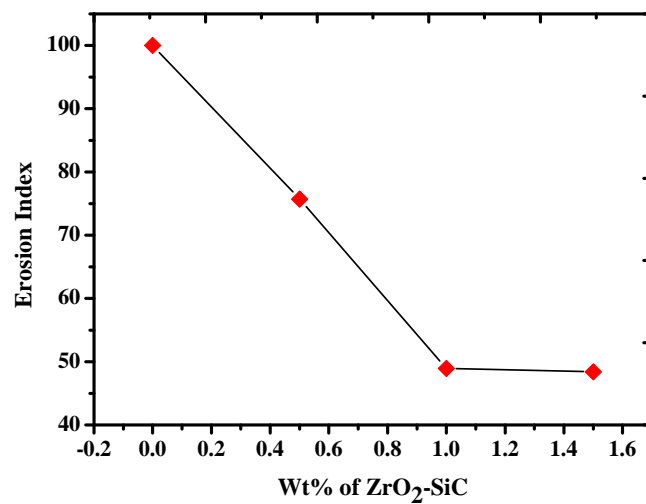


Fig.5.16 Erosion index as a function of wt % of $\text{ZrO}_2\text{-SiC}$ in $\text{Al}_2\text{O}_3\text{-C}$ sample.

5.4 Nitride bonded Al_2O_3 Refractory

The samples T-1, T-2, T-3, T-4 and T-5 were fired under Nitrogen atmosphere at 1600°C for 3 hours. This firing was done to provide the nitride bonds in the material for enhancement of physical and thermo-mechanical properties.

5.4.1 Physical properties

5.4.1.1 Apparent porosity and bulk density

Fig 5.17 shows the variation in physical properties such as AP and BD of samples T-1, T-2, T-3, T-4 and T-5 fired at 1600°C in nitrogen atmosphere.

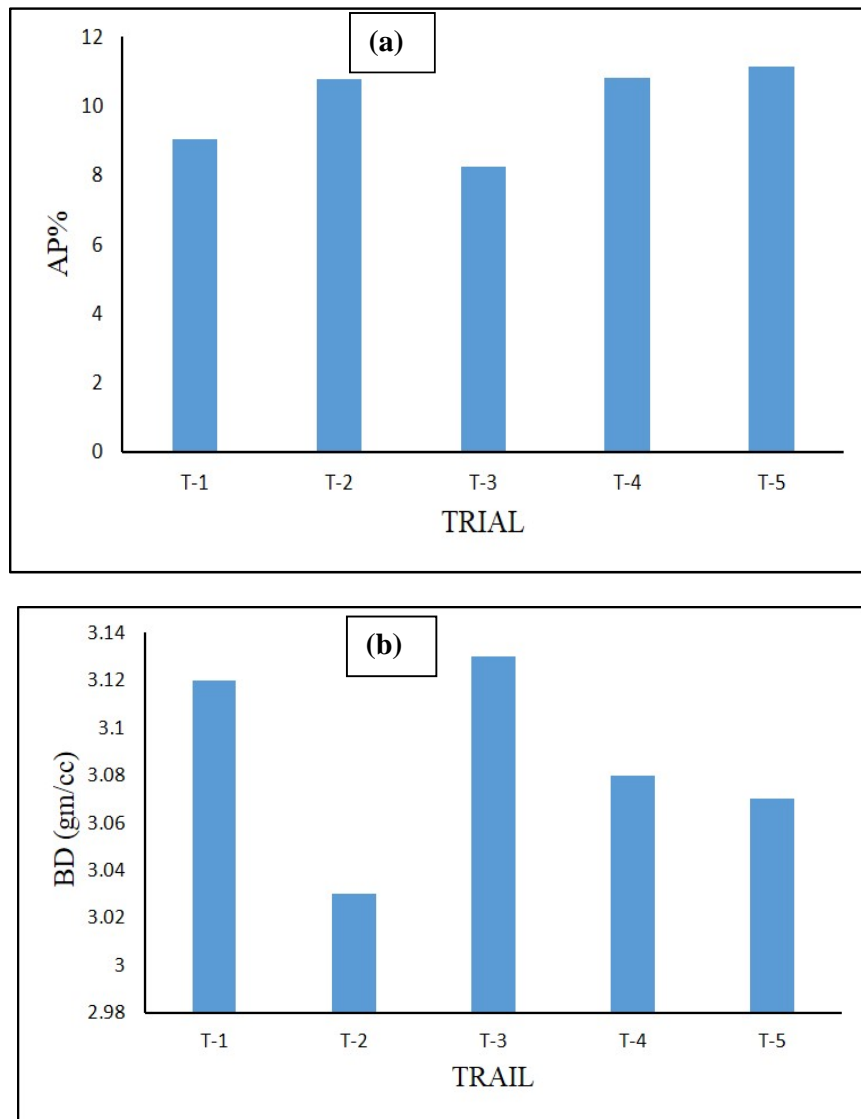


Fig: 5.17 Variation in (a) AP and (b) BD of Al_2O_3 samples fired under N_2 atmosphere.

The apparent porosity values are considerably found better at 1600°C. The excellent value of apparent porosity was found in the sample T-3 with 8.26 % and also T-1 with 9.03%. These two samples are having metals in combination. So the composition with metals in combination were showing better results. Also the composition with only Al metal was showing better result than the composition with only Si metal. The maximum value of BD was seen in the compositions with metals in combination. T-3 having bulk density of 3.13 gm/cc was the highest. It was observed that white fused alumina compositions were showing better properties than tabular alumina samples. To find the reason for better AP and BD, the phase analysis of these samples was analysed.

5.4.2 Structural and microstructural properties

5.4.2.1 Structural properties

Fig 5.18 (a) shows the XRD patterns of samples T-1 (Tabular Alumina) and T-3 (white fused Alumina). For both the samples major peaks are of corundum. Both T-1 and T-3 were having metals in combination. The formation of Sialon was observed in both T-1 and T-3. In XRD, the angle corresponds to the formation of $\text{Si}_4\text{Al}_2\text{O}_2\text{N}_6$ (β -sialon) are 33.29 ° and 35.50 °. This sialon was the reason behind the enhancement of properties in T-1 and T-3 sample. Addition to Sialon, minute amount of AlN was also identified. Figure 5.18 (b) shows the XRD patterns of Al_2O_3 samples T-2 and T-4. In these two samples, only Al metal was added with tabular alumina (T-2) and white fused alumina (T-4). In these two samples, AlN was formed along with the major peaks of corundum. Fig 5.18 (c) shows the XRD patterns of sample T-5 fired in nitrogen atmosphere. The sample T-5 was having only silicon metal. In this sample silicon nitride and also disilicon dinitride oxide formation was observed along with corundum.

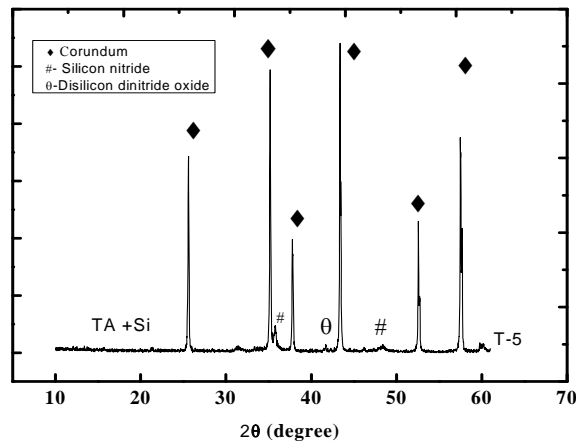
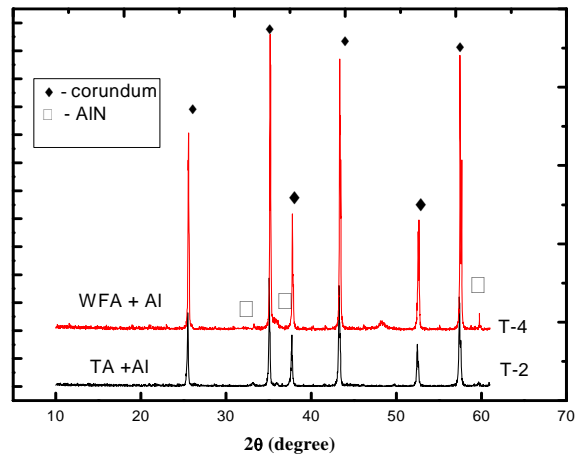
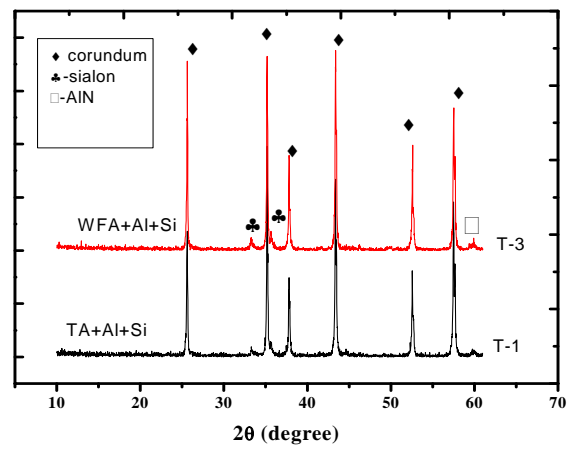


Fig.5.18 XRD patterns T-1, T-2, T-3, T-4 and T-5 fired at 1600°C in N_2 atmosphere.

The excellent AP and BD result of compositions with metal in combination was due to the formation of sialon. Formation of sialon ($\text{Si}_4\text{Al}_2\text{O}_2\text{N}_6$) enhances the strength of the material. The reaction for forming sialon will increase the bonding force between the matrix and the particles^[4]. Sialon is formed by the dissolution of Al and oxygen in silicon nitride. In the samples T-2 and T-4 shows better AP and BD result due to the formation of nitride. In the sample T-5, silicon nitride and silicon oxy nitride are formed. The improvement in properties was due to the formation of nitrides in all the samples.

5.4.3 Thermo-mechanical properties

5.4.3.1 Hot modulus of rupture

Variation in HMOR of the samples fired at 1600°C was shown in Fig 5.19.

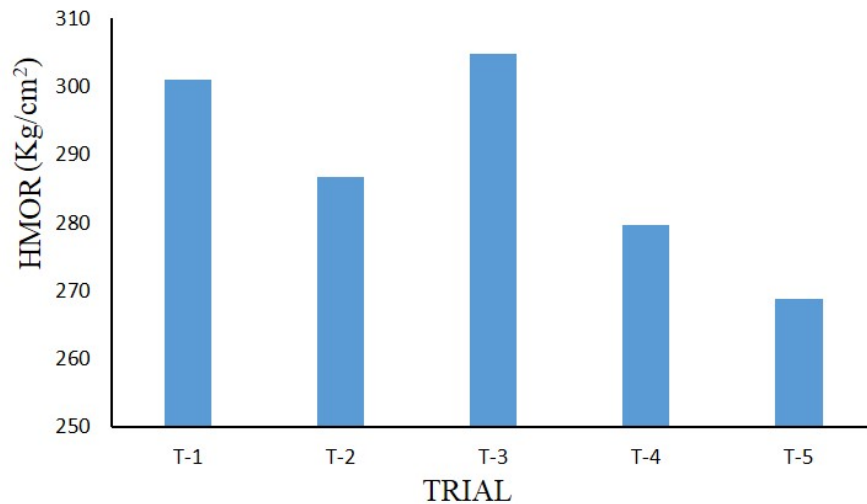


Fig: 5.19 Variation in HMOR for samples T-1, T-2, T-3, T-4 and T-5 fired at 1600°C in Nitrogen atmosphere

From the graph, it was observe that excellent HMOR values were obtained by the samples fired in nitrogen atmosphere. The sample T-3 was showing the maximum value of 304.8 kg/cm² and also T-1 having 301.02 kg/cm². In these samples the enhancement in thermo mechanical property was made possible by the formation of sialon. Presence of sialon would improve the properties of the material. β -Sialon is formed by the reaction between Al_2O_3 , N, Si and Al. The bonding forces between the

matrix and particles, enhanced by this reaction might be the major reason for improvement in HMOR ^[53]. Also in the case of other compositions like T-2, T-4 and T-5, nitride formation was the reason behind increase in thermo –mechanical property.

5.4.3.2 Micro-structural properties

5.4.3.2.1 FESEM (Mapping)

Figure 5.20 (a) shows the FESEM micrograph of sample T-3 fired at 1600°C in nitrogen atmosphere. This composition was having white fused alumina and combination of metals, Al, Si. After firing in nitrogen atmosphere, β -Sialon formation was identified in the microstructure. For confirming the formation of β -Sialon ($\text{Si}_4\text{Al}_2\text{O}_2\text{N}_6$) EDS mapping was performed. Figure 5.20 (b) shows the EDS mapping of the sample T-3. In mapping different colours will represent different elements of the composition. From EDS mapping, it was observed that β -Sialon ($\beta\text{-Si}_4\text{Al}_2\text{O}_2\text{N}_6$) was found in planar structure.

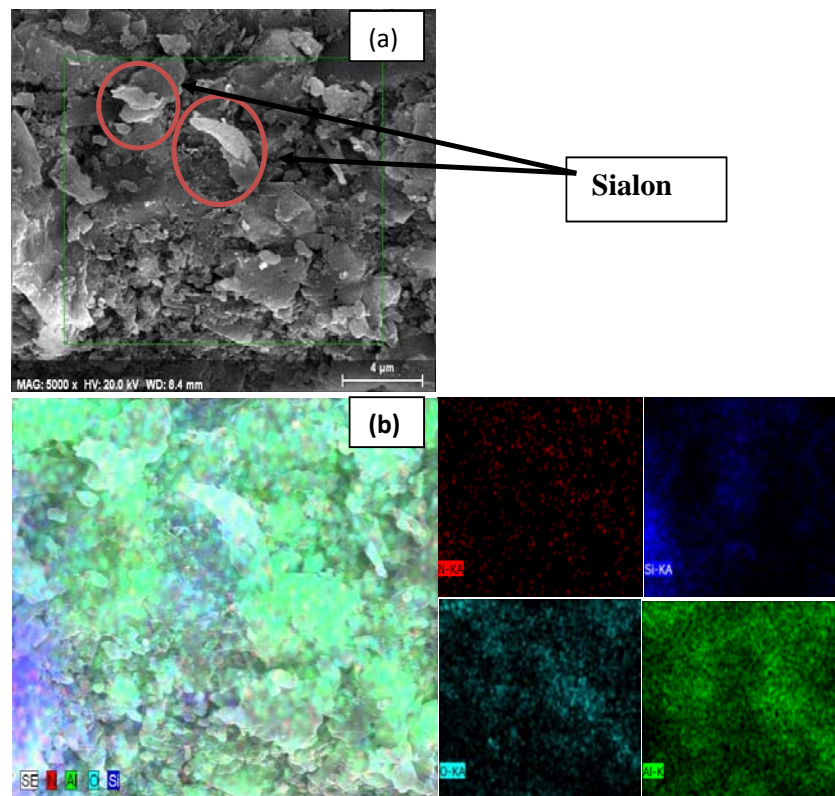


Fig 5.20 FESEM micrograph (a), EDS Mapping (b) of sample T-3.

Chapter -6
Conclusions and scope of future work

- Metal addition in combination of Al and Si has better thermo-mechanical properties than either aluminium added plates or silicon added plates.
- A physical and thermo-mechanical property of plates added with aluminium metal was better than silicon metal added plates.
- Base material with white fused alumina was showing slightly better mechanical and thermo-mechanical properties than TA.
- Composition with white fused alumina and combination of metals has been added with different percentage and form of carbon to study the impact of carbon on physical, thermal and thermo-mechanical properties.
- Less carbon added plates show superior thermo-mechanical properties.
- Addition of both form of carbon has superior thermo-mechanical properties then only addition of carbon black irrespective added amount of carbon.
- Composition with white fused alumina, combination of both metals added with 1.5% carbon black and 1.5% graphite was selected for addition of plasma fused $\text{ZrO}_2\text{-SiC}$ addition to find out the impact of addition and optimization of quantity.
- With the increase in $\text{ZrO}_2\text{-SiC}$ content thermo mechanical properties increase and in all cases thermo-mechanical properties were better than plates without addition of $\text{ZrO}_2\text{-SiC}$.
- Pyro chemical evaluation in form of simulative testing indicates corrosion and erosion resistance improves with the addition of $\text{ZrO}_2\text{-SiC}$ and it improves with the increase in addition of $\text{ZrO}_2\text{-SiC}$ as indicated by the erosion index. No appreciable improvement in erosion index was found beyond 1% addition of $\text{ZrO}_2\text{-SiC}$.
- Nitridisation at 1600°C shows improved physical and thermo mechanical properties irrespective of base material and added metal content.
- However the metal added in combination shows better thermo mechanical properties than plates either added with aluminium metal or silicon metal.
- Plates added with aluminium metal shows better thermo-mechanical properties than silicon metal added plate after Nitridisation.

From these experiments, it was inferred:

- A. Metal bonded plate can be a better substitute than carbon bonded plates for bigger size ladle where spalling is not a problem due to superior strength at high temperature.
- B. White fused alumina is better than White tabular alumina as a base material as white fused alumina has superior resistance to corrosion and has better physical and thermo- mechanical properties due to higher crystal size and grain bulk density resulting in improved packing density.
- C. Metal in combination shows superior performance due to formation of Al_4SiC_4 after firing in both metal bonded and carbon bonded plates and can be a potential material for all type application.
- D. $\text{ZrO}_2\text{-SiC}$ addition further improves the physical and thermo mechanical properties as this addition works as a seeding for carbide formation.
- E. ZrO_2 addition works as a oxygen donor for the formation of oxy carbide bonding.
- F. $\text{ZrO}_2\text{-SiC}$ addition also improves resistance to corrosion as indicates by rotary drum test due to superior properties and as zirconia has superior resistance to corrosion by high basicity slag compared to alumina.
- G. Nitridisation of metal bonded plates improves the physical and thermo mechanical properties due to formation of nitride/oxy nitride/sialon in the matrix and can be potential material for future for application as insert in slide gate plate.

Scope of future work		2014
----------------------	--	-------------

- $\text{ZrO}_2\text{-SiC}$ of different mesh size can be tried for optimisation.
- Also higher percentage of $\text{ZrO}_2\text{-SiC}$ can be incorporated for further studies.
- Further work on sialon bonding is required to, optimise firing temperature and addition of catalyst.
- Field trial is required to correlate the properties with actual performance.

References

- [1] R. Amavis, "*Refractories for The Steel Industry*," Elsevier Science, London (1990).
- [2] H. Lax, "*The Use of Refractories in Continuous Casting Plants*," Interceram, Special Issue (1987).
- [3] H. Shikano, "*Refractories Handbook*," Technical Association of Refractories, Japan (1998).
- [4] J. Javadpour, H. R. Rezaie, R. Naghizadeh, "*Effect of additives on the properties and microstructures of Al₂O₃-C refractories*," J. Mater. Sci. 41(2006) 3027–3032.
- [5] C. TAFFIN and J. POIRIER, "*The behaviour of metal additives in MgO-C and Al₂O₃-C refractories*," Interceram 43 5 (1994) 354.
- [6] A. YAMAGUCHI, "*Thermochemical analysis of reaction processes of aluminium and aluminium-compounds in carbon-containing refractories*," Taikabutsu Overseas 7 2 (1987) 11-16.
- [7] Annual book of ASTM standards, "*Refractories: Activated carbon, Advanced ceramics*," 15.01, pp.19 (2003).
- [8] Kingery W.D, Bowen H.K, Uhlmann D.R, "*Introduction to ceramics*," John Wiley and sons, New York, (1975).
- [9] Chester J.H, "*Refractories production and properties*," The iron and steel institute, Carlton house Terrace London (1973), pp(10-11).
- [10] "*MPT International*" Volume 30 (2007), issue No. 6.
- [11] Haibing Fan, Yawei Li, Shaobai Sang, "*Microstructures and mechanical properties of Al₂O₃-C refractories with silicon additive using different carbon sources*," Materials Science and Engineering A 528 (2011) 3177–3185.
- [12] Advanced seminar on refractories for steel making, 2005, pp(68-69).
- [13] Lj. Kljajevi, B. Matovi, A. Radosavljevi-Mihajlovi, M. Rosi, S. Boskovi, A. Devecerski, "*Preparation of ZrO₂ and ZrO₂/SiC powders by carbo-thermal reduction of ZrSiO₄*," Journal of Alloys and Compounds 509 (2011) 2203–2215.
- [14] Haibing Fan, Yawei Li, Yupeng Huang, Shaobai Sang, Yuanbing Li, Lei Zhao, "*Microstructures and mechanical properties of Al₂O₃-ZrO₂-C refractories using silicon, microsilica or their combination as additive*," Materials Science and Engineering A 545 (2012) 148– 154
- [15] S. Zhang .*UNITECRCongressUSA2* (1997)861.
- [16] T. Kawakami, K. Aratani, S. Hasegawa, T. Sato, *Taikabutsu Overseas* 8 (3) (1988) 18.
- [17] Liu Qing-cai, Zheng Hui-min, Lu Cun-fang, Gao Wei "*Corrosion resistance of high-alumina graphite based Refractories to the smelting reduction melts*," Journal of Materials Science and Engineering, 2 (2008) ISSN1934-8959.
- [18] Ming Luo, Yawei Lin, Shaobai Sang, Lei Zhao, Shengli Jin, Yuanbing Li, "*Microstructure and mechanical properties of multi-walled carbon nanotubes containing Al₂O₃-Crefractories with addition of polycarbosilane*," Ceramics International 39(2013) 4831–4838.

- [19] MaBei-yue, Yu Jing-ku, "Synthesis of ZrO_2 -SiC composite powder and effect of its addition on properties of Al_2O_3 -Crefractories," Trans. Nonferrous Met. SOCC. Hina 17 (2007) 996-1000.
- [20] K. Sasai, Y. Mizukami., "Reaction Rate between Alumina Graphite Immersion Nozzle and Low Carbon Steel," ISIJ International, 35 (1995) 1 26-33.
- [21] Liu Q. C, "Reduction rate of ferrous oxide in smelting Reduction," Journal of Iron and Steel Research, 1998, 5(4):17-20.
- [22] Q. C, "Study on foaming behaviour of molten slag during smelting reduction with iron bath," Journal of Iron and Steel Research, 1996, 3(2): 7-10.
- [23] S.Q. Zheng, G.H.Min, Z.D. Zou, C. Tatsuyama, "High temperature oxidation of calcium hexaboride powders," J. Mater Lett, 58 21 (2004) 2586-2589.
- [24] Y.Q. Li, T. Qiu, "Oxidation behaviour of boron carbide powder," Mater. Sci. Eng .A, 2007, 444(1/2) 184-197.
- [25] Yu J. K, "Improvement of the corrosion resistance of refractories by adding Al_2O_3 -SiC composites synthesized from natural minerals," J. Taikabutsu, 1997, 49 (11) 607.
- [26] Yin Zhu Jiang, Jianfeng Gao, Mingfei Liu, Yanyan Wang, Guangyao Meng, "Fabrication and characterization of Y2O3 stabilized ZrO_2 films deposited with aerosol-assisted MOCVD," J. Solid State Ionics, 2007, 177 (39/40): 3405-341 0.
- [27] Y. Yang, K. Yang, Z.M. Lin, J.T. Li, "Mechanical-activation-assisted combustion synthesis of SiC," Mater Lett, 2007, 61 (3) 671-676.
- [28] C.G. Aneziris, U. Klippel, W. Schärfl, V. Stein, Y.W. Li , Int. J. Appl. Ceram. Technol. 4 (6) (2007) 489–1489.
- [29] C.G. Aneziris, D. Borzov, J. Ulbricht, "Magnesia Carbon bricks –A high duty brick material ,," Interceram (2003) 22–27.
- [30] E. Mohamed, M. Ewais, "Carbon based refractories," J Ceram Soc Jpn, 2004, 112(10) 517-532.
- [31] C.F. Cooper, I.C. Alexander, C.J. Hampson, " The Role of Graphite in the Thermal Shock Resistance of Refractories," Br. Ceram. Trans. J. 84 (2) (1985)57–62.
- [32] M.N. Khezrabadi, J. Javadpour, H. R. Rezaie, R. Naghizadeh, "The effect of additives on the properties and microstructures of Al_2O_3 -C refractories," J. Mater. Sci. 41 (2006) 3027–3032.
- [33] S. Zhang , J. Eur. Ceram. Soc. 21 (2001) 1037–1047.
- [34] M. Hassanet, Composites A 35 (2004)519–527.
- [35] R.W. Rice I, Ceram. Eng. Sci. Proc. 2 (7/8) (1981) 661–701.
- [36] K.A. Trick , Carbon 33 (11) (1995) 1509–1515.
- [37] N.I. MakarevichI, J. Appl. Spectrosc. 26 (4) (1977) 531–535.
- [38] J.G. Wang, Q.G. Guo, L. Liu, J.R. Song, Carbon 40 (2002) 2447–2452.
- [39] E. Bafekrpour, P.S. George, J. Habsuda, M. Naebe, C.H. Yang, F. Bronwyn, Mater. Sci. Eng. A. 545 (2012) 123–132.
- [40] H.Y. Jiang, J.G. Wang, S.Q. Wu, B.S. Wang, Z.Z. Wang, Carbon 48 (2010) 352–358.

- [41] Ming Luo, Yawei Lin, Shaobai Sang, Lei Zhao, Shengli Jin, Yuanbing Li *et al* “*In situ formation of carbon nanotubes and ceramic whiskers in Al₂O₃–C refractories with addition of Ni-catalyzed phenolic resin,*” Materials Science & Engineering A 558 (2012) 533–542.
- [42] Heng Wang, Yawei Li, Tianbin Zhu, Shaobai Sang, Qinghu Wang, “*Microstructures and mechanical properties of Al₂O₃–C refractories with addition of microcrystalline graphite,*” Ceramics International (2014).
- [43] C.G. Aneziris, V. Rountos, “*Interactions of carbon nanotubes in Al₂O₃–C refractories for sliding gate applications,*” UNITECR, Brazil, 2009, p. 8.
- [44] Ming Luo, Yawei Li, Shengli Jin, Shaobai Sang, Lei Zhao, Yuanbing Li *et al*, “*Microstructures and mechanical properties of Al₂O₃–C refractories with addition of multiwalled carbon nanotubes,*” Mater. Sci. Eng. A 548 (2012) 134–141.
- [45] Pavol Hvizdos, Jan Dusza, Csaba Balazsi, “*Tribological properties of Si₃N₄–grapheme nanocomposites*”, J. Eur. Ceram. Soc. 33 (2013) 2359–2364.
- [46] Kai Wang, Yongfang Wang, Zhuangjun Fan, Jun Yan, Tong Wei, “*Preparation of grapheme nanosheet/alumina composites by spark plasma sintering*”, Mater. Res. Bull, 46 (2011) 315–318.
- [47] A. Centeno, V.G. Rocha, B. Alonso, A. Fernandez, C.F. Gutierrez-Gonzalez, R. Torrecillas, A. Zurutuza, “*Graphene for tough and electroconductive alumina ceramics*”, J. Eur. Ceram. Soc. 33 (2013) 3201–3210.
- [48] Tianbin Zhu, Yawei Li, Ming Luo, Shaobai Sang, Qinghu Wang, Lei Zhao, Yuanbing Li, Shujing Li, “*Microstructure and mechanical properties of MgO–C refractories containing graphite oxide nanosheets (GONs)*”, Ceram. Int. 39 (2013) 3017–3025.
- [49] Q.H. Wang, Y. Li, M. Luo, Shaobai Sang, T. Zhu, L. Zhao, “*Strengthening mechanism of graphene oxide nanosheets for Al₂O₃–C refractories,*” Ceram. Int. 40 (2014) 163–172.
- [50] Steffen Dudczig, Daniel Veres, Christos G. Aneziris, Erik Skiera, Rolf W. Steinbrech, “*Nano- and micrometre additions of SiO₂, ZrO₂ and TiO₂ in fine grained alumina refractory ceramics for improved thermal shock performance,*” Ceram. Int. 38 (2012) 2011–2019.
- [51] C.G. Aneziris, J. Hubalkova, R. Barabas, “*Microstructure evaluation of MgO–C refractories with TiO₂- and Al-additions,*” J. Eur. Ceram. Soc. 27 (2007) 73–78.
- [52] Qinghu Wang, Yawei Li, Ming Luo, Shaobai Sang, Tianbin Zhu, Lei Zhao, “*Strengthening mechanism of grapheme oxide nanosheets for Al₂O₃–C refractories,*” Ceramic international 40 (2014) 163–172.
- [53] Boquan Zhu, Yuenan Zhu, Xiangcheng Li, Fei Zhao, “*Effect of ceramic bonding phases on the thermo-mechanical properties of Al₂O₃–C refractories,*” Ceramics International 39 (2013) 6069–6076.
- [54] Xiangcheng Li, Boquan Zhu, Yuenan Zhu, “*Alumina–carbon refractories strengthened by insitu synthetic O–SiAlON whiskers,*” China’s refractories 40 (6) (2006) 415–418.